REPORT

Groundwater flow in the Ischia volcanic island (Italy) and its implications for thermal water abstraction

Vincenzo Piscopo[1] · Francesca Lotti[2] · Fulvio Formica[3] · Luigi Lana[2] · Luigi Pianese[3]

Abstract
This study improves knowledge on the hydrogeology of Ischia Island, an active volcano of southern Italy. Combining previous published and unpublished data with newly collected data, and through the results of simplified numerical models, the existing conceptual hydrogeological model of the volcanic island has been reviewed and the present impact of intensive withdrawals on the island's groundwater resources has been examined. Two areas with different hydrogeological characteristics have been recognized: (1) the resurgent block of Mt. Epomeo, where an independent and uplifted basal groundwater circulation exists; (2) the external areas of Mt. Epomeo, where a continuous basal aquifer and local discontinuous perched aquifers have been distinguished. The marginal faults of the resurgent block of Mt. Epomeo represent the preferential pathways of ascending deep fluids. In natural conditions, the island's aquifers are recharged by rainfall and by deep fluids from beneath, discharging towards the sea and the springs. Since the start of activity at the spa facilities, involving intensive pumping from wells, a further and significant recharge of the aquifers has come from seawater and from increased upwelling of the deep fluids. Although this does not compromise the sustainability of the groundwater withdrawals in quantitative terms, the pumping rates determine the quality of the water captured by the wells. The great variability in temperature and chemical composition of groundwater of the island is also influenced by local hydrogeological parameters and characteristics of the wells from which the water samples were taken, as well as the phenomena of interaction among different end-members.

Keywords Volcanic aquifer · Thermal groundwater · Conceptual model · Intensive use · Italy

Introduction

Ischia is one of the active volcanic islands in Italy (Fig. 1) and it has been the subject of volcanological, petrographic, geochemical and geophysical studies, which are widely reported in the literature. In particular, the hydrothermal system of the island (whose surface manifestations are thermal waters, fumaroles and steaming grounds) has been the subject of numerous scientific notes, given also the implications for geothermal energy and the volcanic hazard assessment (the relevant literature is cited in the following). On the other hand, few

✉ Vincenzo Piscopo
piscopo@unitus.it

[1] Dipartimento di Scienze Ecologiche e Biologiche, Università degli Studi della Tuscia, Viterbo, Italy

[2] Kataclima, Vetralla, VT, Italy

[3] Acque Terme Ambiente Consulting, Naples, Italy

hydrogeological studies have been published, although the island's economy depends principally on groundwater.

The Island of Ischia (surface area of about 46 km^2) is a famous tourist resort for spa treatments. There are 290 hotels, 70% of which have spas. The municipalities of Ischia and Forio register the largest number of accommodation facilities. In 2016, these two municipalities hosted about 2.6 million tourists, equivalent to 0.6% of the total tourist flow of Italy (ISTAT 2017). The spas are supplied by withdrawals mainly from wells and secondarily from springs. According to a recent census of Regione Campania (the regional public body that grants licenses to use thermal and mineral waters), there are 264 groundwater tapping points on the island (244 wells and 20 springs; Regione Campania, unpublished report, 2015), located in an area of about 18 km^2 mainly near the coast.

The observed wide ranges of the groundwater chemical composition (from calcium-bicarbonate to alkali-chloride waters; Fig. 1), salinity (from 1 to 42 g/L) and temperature (from 13 to 90 °C) have been explained by different geochemical
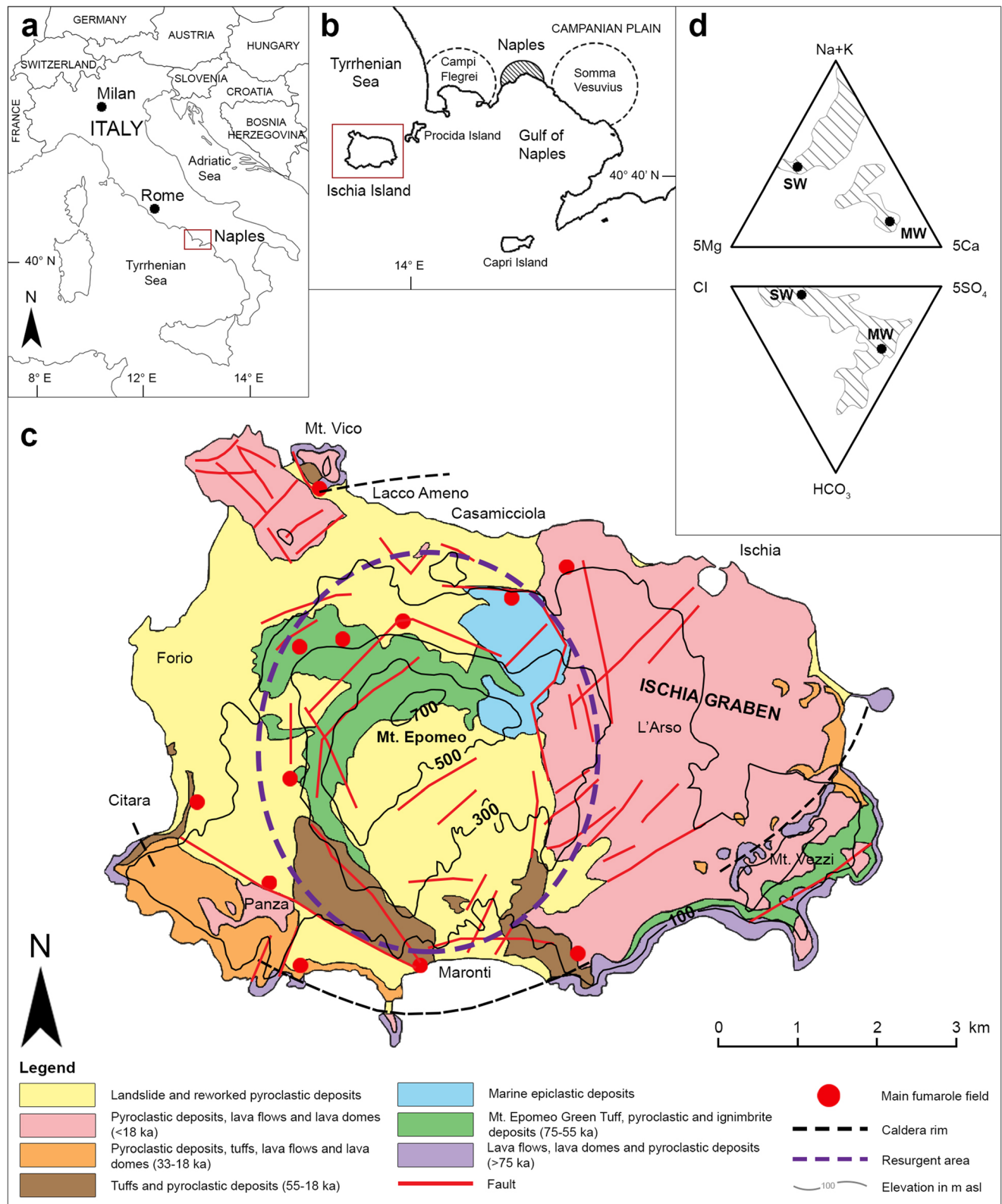
Fig. 1 **a** Location of the Island of Ischia in the Italian Peninsula and **b** in the Gulf of Naples, **c** simplified geologic map of Island of Ischia (surface geology modified from Sbrana and Toccaceli 2011; structural lineaments modified from Della Seta et al. 2012), **d** range of dissolved major ions in the groundwaters, in Na + K – 5 Mg – 5Ca and Cl – 5SO$_4$ – HCO$_3$ triangular plots (SW seawater, MW meteoric water; from Di Napoli et al. 2009)

models including mixing processes among meteoric water, seawater and deep geothermal fluids, and water–rock interactions (De Gennaro et al. 1984; Panichi et al. 1992; Aiuppa et al. 2006; Di Napoli et al. 2009).

While information on the geochemical features of the groundwater is detailed, there is not such a degree of knowledge on the groundwater flow. In the few available hydrogeological studies, two distinct hydrogeological sectors, coinciding with the main volcano-tectonic structures of the island, can be recognized (Fig. 1): "Ischia graben", characterized by a single aquifer recharged by both rainfall and seawater intrusion, and "Mt. Epomeo horst" and its margins, where a less transmissive and more heterogeneous aquifer has been found. In this last sector, the aquifer is recharged by rainfall, seawater intrusion and rising geothermal fluids (Celico et al. 1999). The hydrogeological studies also indicate that the relationships between meteoric recharge, seawater intrusion and deep fluids are influenced by the pumping that supplies the spas (Celico et al. 1999; Piscopo et al. 2000; Baiocchi et al. 2017).

This study is aimed at improving knowledge on the hydrogeology of Ischia, combining previous published and unpublished data with new data collection, analysis and numerical processing. The main objectives are to review the existing conceptual hydrogeological model of the volcano (Celico et al. 1999) and to examine the present impact of intensive abstraction of the island's groundwater resources. This topic is fundamental for planning sustainable management of the island's groundwater resources, on which the local economy depends. At the same time, the case study represents an opportunity to deepen the knowledge on the hydrogeology of active volcanoes, which is also essential for the development and correct interpretation of an effective hazard monitoring system (Shibata and Akita 2001; Hurwitz and Johnston 2003; Hurwitz et al. 2003; Revil et al. 2011) and to understand the role of groundwater in volcanic processes (Reid et al. 2001; Join et al. 2005; Fournier et al. 2010).

Volcanological, structural and hydrothermal features of Ischia

The Island of Ischia is in the Neapolitan volcanic area (Fig. 1), located in a Pliocene-Quaternary peri-Tyrrhenian graben of the Apennine Chain, where a crustal thinning produced intense volcanic activity since the early Pliocene (Scandone 1979). Volcanism initially gave rise to rocks varying in composition from calc-alkaline andesite-basalts and andesite, and later to potassic-alkaline volcanites (Di Girolamo et al. 1984; Beccaluva et al. 1991; D'Antonio et al. 2007). The latest manifestations of volcanism of the Neapolitan area are the three active volcanoes of Ischia (150 ka to AD 1302), Campi Flegrei

(58 ka to AD 1538) and Somma-Vesuvius (22 ka to AD 1944; Santacroce et al. 2003).

The Island of Ischia constitutes the emerged part of a wider volcanic edifice of the Gulf of Naples, which also includes Procida Island and Campi Flegrei (Fig. 1), and represents an active resurgent caldera in this volcanic district (Orsi et al. 1996). Ischia is composed of volcanic rocks (Fig. 1), ranging in composition from shoshonite to latite, trachyte and phonolite, epiclastic deposits, marine sediments and landslide deposits (Vezzoli 1988; Crisci et al. 1989; Civetta et al. 1991; Orsi et al. 1992; de Vita et al. 2006; Sbrana and Toccaceli 2011; Della Seta et al. 2012). Pyroclastic deposits with paleosols outcropping in the southeastern sector of the island represent the oldest products (prior to 150 ka). The volcanic activity between 150 and 75 ka gave rise to trachytic to phonolitic lava domes, and secondarily alkali-trachytic pyroclastic deposits, outcropping in the peripheral sectors of the island. Between 75 and 33 ka, the island was affected by the most remarkable eruptions, among which the largest one was the Mt. Epomeo Green Tuff eruption (55 ka) accompanied by the caldera collapse (Vezzoli 1988; Tibaldi and Vezzoli 1998). Mt. Epomeo Green Tuff eruption gave rise to a large volume of ignimbrite fed by trachytic to phonolitic magma. The resulting collapse of the caldera led to the flooding of its floor by the sea and filling with marine sediments and epiclastic deposits. Later, a resurgence phenomenon started within the caldera producing over time an uplift of the Mt. Epomeo block of about 900 m (Orsi et al. 1991). The volcanological history of the island after the Mt. Epomeo Green Tuff eruption is divided into three periods of activity. The first period continued up to 33 ka with phreatomagmatic and magmatic explosive eruptions by trachytic to phonolitic magma. The second period, developed between 30 and 18 ka, began with eruption fed by shoshonitic magma and followed by effusive and explosive activity, mainly in the southwestern sector, fed by trachytic to phonolitic magmas. In the third period, between 10 ka and AD 1302, the volcanic activity mostly took place within the eastern sector of the island controlled by an extensional stress regime related to the resurgence phenomenon. Initially, small-size lava effusions as well as phreatomagmatic and magmatic explosive eruptions, fed by differentiated magmas, occurred. At about 6 ka, volcanic activity occurred also in the northwestern sector of the island. The last phase of uplift of Mt. Epomeo block (8.6–5.7 ka) was accompanied by slope instability and landslide formations all around the relief. Further intense phases of activity concerned the eastern sector at 5.5 and 3 ka; the latter included 35 eruptions and ended in AD 1302 with Arso eruption (Civetta et al. 1991; Orsi et al. 1991; Vezzoli et al. 2009; de Vita et al. 2010).

The structural setting of the island is related to interactions between the resurgence of the Mt. Epomeo block and regional tectonics. Four main fault systems have been recognized (Fig. 1). ENE–WSW to E–W and NNW–SSE

to N–S striking systems surround the Mt. Epomeo resurgent block. NE–SW and NW–SE striking systems, related to regional tectonics, control the eastern, northwestern and southwestern structures of the island (Orsi et al. 1991; Acocella and Funiciello 1999; Molin et al. 2003; Della Seta et al. 2012). The peripheral structures of Mt. Vezzi in the SE, Panza in the SW, and Mt. Vico in the NE represent morphologic highs where volcanic products pre-Mt. Epomeo Green Tuff outcrop (Fig. 2). The lowered structure of the Ischia graben, between the structural highs of Mt. Epomeo and Mt. Vezzi, houses the most recent volcanic products of the eastern sector (Vezzoli 1988).

The uplift of Mt. Epomeo has been interpreted through different genetic models that agree on the induced deformation of a shallow magmatic body, whose top is located at a depth of about 2 km (Vezzoli 1988; Orsi et al. 1991; Tibaldi and Vezzoli 2004; Paoletti et al. 2009; Carlino 2012; Carlino et al. 2014). This magmatic body is the origin of an active geothermal system whose surface manifestations are the hot waters, fumaroles and steaming grounds of the island (Fig. 2). A wide range of chemistry characterizes the waters of wells and springs, with temperatures between 13 and 90 °C, salinity between 0.76 and 42 g/L, composition variable from calcium-bicarbonate to alkali-chloride (Fig. 1), and concentration of the dissolved CO_2 between 1 and 448 cm^3/L (Di Napoli et al. 2009).

Many geochemical studies conducted on the waters and fumaroles of the island have highlighted the presence of a complex hydrothermal system due to overlapping and interconnected reservoirs fed by meteoric waters, seawater and magma-derived or mixed magmatic-crustal gases. The release of gas also occurs from soil and fumaroles (De Gennaro et al. 1984; Carapezza et al. 1988; Panichi et al. 1992; Tedesco 1996; Caliro et al. 1999; Inguaggiato et al. 2000; Chiodini et al. 2004; Aiuppa et al. 2006). Through more recent and complete geochemical investigations, Di Napoli et al. (2009) explain the great variability in the physico-chemical parameters, isotopic compositions and gas contents of groundwater as complex mixing among different end-members: meteoric water, seawater and three thermal end-members. The eastern sector of the island (i.e., in the Ischia graben, Fig. 1) is the only place where groundwater can be related to a mixing between meteoric water and seawater. In the other sectors of the island, groundwater compositions are altered by water–rock interaction and evaporative processes, in addition to meteoric-seawater-mixing phenomena. The same authors (Di Napoli et al. 2009), on the basis of the estimated deep equilibrium temperatures, distinguish: a shallow hydrothermal reservoir (150–300 m deep) in the southern and western sectors of the island with estimated equilibrium temperature of about 150 °C, mainly recharged by meteoric and marine fluids; a deep hydrothermal reservoir (>300 m deep, but possibly
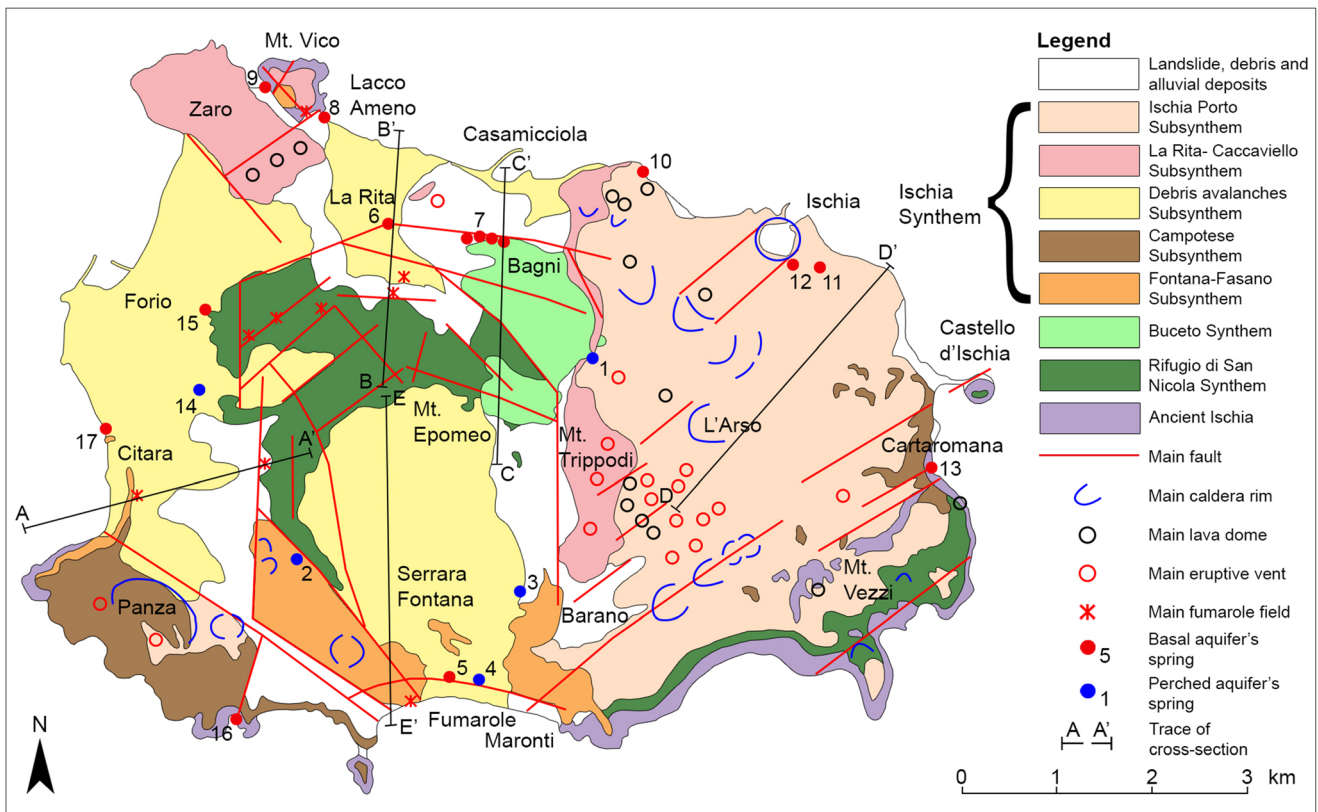

Fig. 2 Geological sketch map of the Island of Ischia (modified from Sbrana and Toccaceli 2011 and Vezzoli 1988) with the location of the main springs

>1,000 m) in the northern and south-western sectors of the island with equilibrium temperatures of 200–270 °C. The ascending of these deep geothermal fluids (referred as deep fluids hereinafter) and mixing with meteoric and seawater explain the chemical and isotopic heterogeneity of groundwaters of the island (namely those present in the first 200 m of depth, intercepted by spa wells). The deep fluids have been related to a large heat and volatile flux due to cooling and degassing of the magmatic body, which supplies the hydrothermal system with $1.2–1.7 \times 10^6$ ton/year of magmatic water (Di Napoli et al. 2009).

Regarding the heat flow affecting the island, an average value of about 500 mW/m^2 was estimated (Carlino et al. 2014). The geothermal gradient of the southern and western sectors of the island ranges from 150 to 250 °C/km. The geothermal system is vapor dominated and a large amount of heat discharge occurs along the faults bordering Mt. Epomeo block (Carlino et al. 2014), representing the preferred pathways for hydrothermal circulation (Molin et al. 2003). Along faults and fractures, the hydrothermal alteration of the volcanic rocks can lead to self-sealing structures, which control the heterogeneity and anisotropy of the hydraulic conductivity and of the temperature distribution (Paoletti et al. 2013).

Investigations and methods

The investigation involved a review of the conceptual hydrogeological model of the volcanic island and mainly included: (1) hydrogeological characterization of the volcanic units, (2) inventory and new flow measurements of springs, (3) wells data acquisition and processing, (4) new water level, temperature and electrical conductivity measurements of selected wells; (5) meteorological data processing.

Hydrogeological characterization of the aquifers of the island hosted in the first 200 m of depth was carried out considering stratigraphy, volcano-tectonic structures, and data of the wells and springs. For stratigraphy, the 1:10,000 scale geological maps of Vezzoli (1988) and Sbrana and Toccaceli (2011) were considered; those authors distinguish 88 and 130 stratigraphic units, respectively. The volcano-tectonic setting was derived from the aforementioned geological maps, as well as from more specific studies (Orsi et al. 1991; Acocella and Funiciello 1999; Molin et al. 2003; de Vita et al. 2010; Paoletti et al. 2013). The stratigraphic and structural data were completed with those deriving from about 200 wells acquired from the literature (Celico et al. 1999; Di Napoli et al. 2009; Carlino et al. 2014), public databases and unpublished technical reports (Regione Campania, unpublished reports, 2007 and 2015). Information regarding wells and boreholes included well depth, aquifer formation, water level and temperature, well discharge and pumping test results. Historical series of piezometric level measurements (performed between the

1930s and 1950s, every 3 days) are available for six wells (Annals of the Italian Hydrographic Service 1929–1994).

In the period between 2014 and 2018, new measurements were performed including: water level (accuracy ±1 cm) and well discharge (accuracy 5%) on 70 selected wells with elevation determination (accuracy ±50 cm); temperature (accuracy ±0.1 °C) and electrical conductivity (accuracy 5%) logs on 19 wells (ranges 0–70 °C and 0–80,000 μS/cm, respectively); flow measurement of the main springs and selected stream sections using tanks or flowmeter (accuracy from 5 to 10%). The wells considered during the surveys pertain to thermal establishments. They do not have a homogeneous distribution on the island and often are not measurable due to surface casing, well seals or extraction devices.

Rainfall and air temperature data for the area were obtained from the Italian Hydrographic Service and Regione Campania. The most complete series of precipitation and air temperature data concern three weather stations of the Italian Hydrographic Service. For these stations, 59 years of daily data are available for the period 1921–1999. They were statistically processed to analyze the homogeneity of the data series by applying the cumulative residuals method, and gaps were filled in to complete the series.

Results

Types of aquifer formation

A first characterization of the aquifer formations was carried out considering the saturated thickness of stratigraphic units intercepted by wells. Six zones with different aquifer formations can be distinguished in the island (Fig. 3): ancient lava aquifer (ALA), uplifted Green Tuff aquifer (GTA), epiclastic deposits and Green Tuff aquifer (ETA), pyroclastic deposits and Green Tuff aquifer (PTA), pyroclastic and lava aquifer (PLA), volcanic and epiclastic aquifer (VEA).

The ALA includes the products older than 75 ka between a few meters above sea level (asl) and a few hundred meters deep (Ancient Ischia in Fig. 2). In south-western, south-eastern and north-eastern peripheral areas of the island, lava domes, lava flows and scoriae prevail on fine pyroclastic deposits at these depths. The few wells present in these areas have a water level from 0 to 1 m asl and deepen for a few tens of meters below it. The hydraulic conductivity of the ALA is mainly due to the secondary porosity of the prevailing lava rocks, which are affected by typical cooling fissures, as well as by NE–SW and NW–SE fault and fracture systems (Fig. 2). It is assumed that fractured lava rocks have significant hydraulic conductivity to a few hundred meters of depth.

The GTA has been distinguished based on stratigraphic and structural setting, indirect subsurface data, and data arising from the few boreholes crossing this aquifer. The GTA
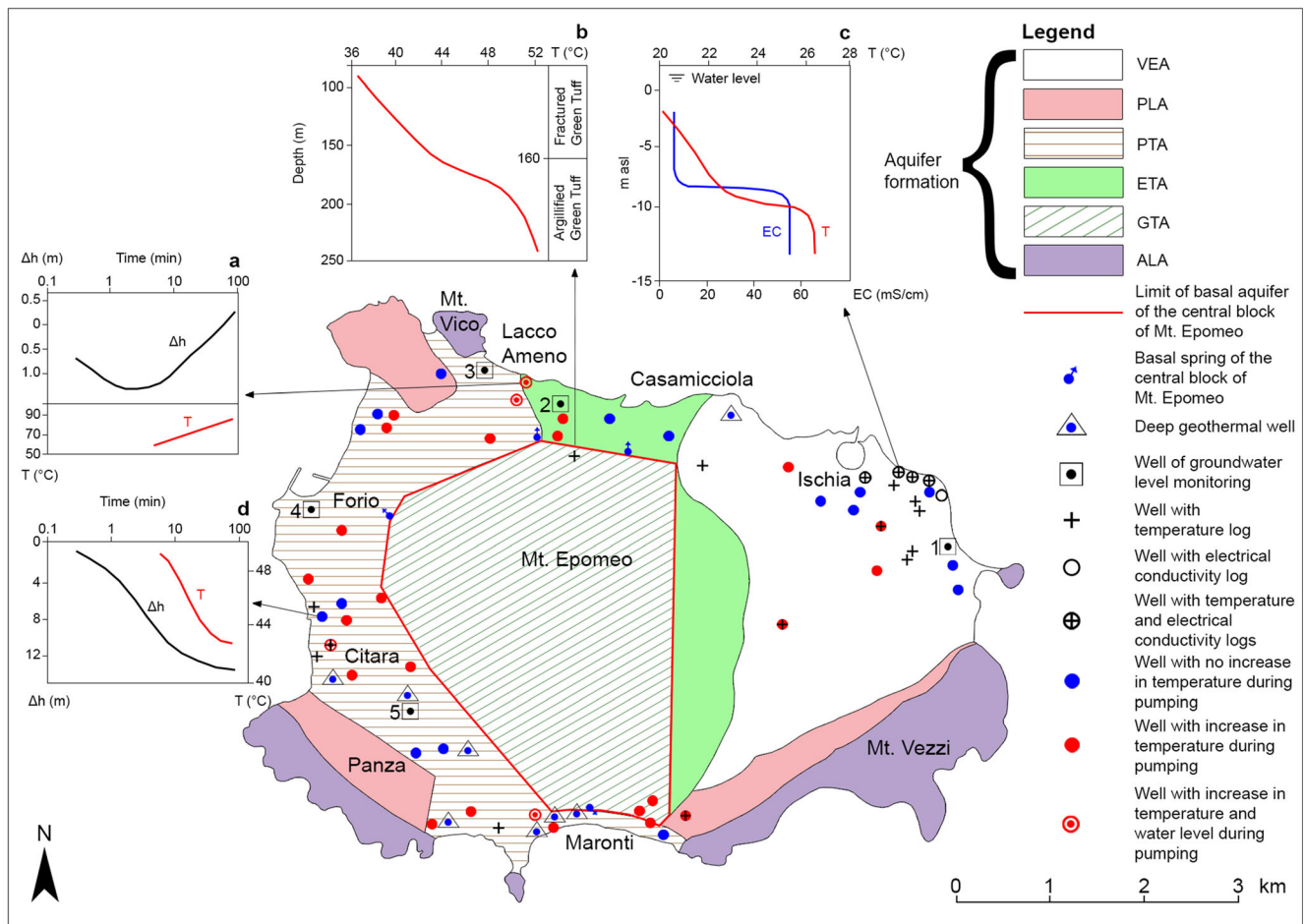
Fig. 3 Map of the aquifer formations with the location of the analyzed wells. **a** Increase in temperature (*T*) and trend of water level (Δ*h*) during pumping (from Celico et al. 1999), **b** temperature log in a well located upstream of the marginal faults of the resurgent block of Mt. Epomeo, **c** temperature (*T*) and electrical conductivity (EC) logs in a well close to the coastline, **d** decrease in temperature (*T*) and trend of water level (Δ*h*) during pumping in a well close to the coastline

constitutes the central sector of the resurgent block of Mt. Epomeo (Fig. 3). In this area, a groundwater flow in the GTA is to be expected, if the following items are considered: (1) the increase of hydraulic head in the bordering aquifers towards the central sector of the island, (2) the presence of a few springs with significant flow in the debris and landslide deposits that cover the GTA, (3) the groundwater level measured in the few wells drilled at the margins of the resurgent block (Fig. 4).

In the central sector of Mt. Epomeo, Vezzoli (1988) recognizes a dense welded ignimbrite, mainly made up of abundant porphyric pumice and xenolith and crystal sets in a scarce vitric matrix, with a maximum thickness of a few hundred meters (Green Tuff of Mt. Epomeo). In the ignimbrite succession of Mt. Epomeo (belonging to Rifugio di San Nicola Synthem in Fig. 2), Sbrana and Toccaceli (2011) distinguish three units interlayered with epiclastic deposits, including from the bottom upwards: a massive welded and intensely welded ash tuff with eutaxitic texture formed by pumice lapilli, crystals and lithic fragments with thickness up to 150 m

(Pizzone Tuff); a massive ash and pumice tuffs, including scoria and lava lithics and breccia layers, with thickness ranging from 50 to 300 m (Frassitelli Tuff); a massive ash and pumice tuff including lithic fragments and crystals with maximum thickness of 200 m (Green Tuff of Mt. Epomeo Auctt., partly). The ignimbrite succession of the central sector of the island is intensely fractured and faulted also due to resurgent block dynamics (Fig. 2). It follows that the hydraulic conductivity of the GTA is due to both primary and secondary porosity, and the hydraulic conductivity due to fractures is to be considered greater than that of the matrix. A decrease in permeability with depth is to be expected due to the pervasive hydrothermal alteration of the ignimbrite succession.

The ETA consists of epiclastic deposits and the underlying ignimbrite units constituting the aquifer formations in the northern and eastern slopes of Mt. Epomeo (Fig. 3). The epiclastic deposits include epiclastic tuffs with an abundant silty and ashy matrix, from massive to stratified and jointed (Mt. Epomeo Tuffite and Colle Jetto Formation in Vezzoli 1988; Buceto Synthem in Sbrana and Toccaceli 2011;
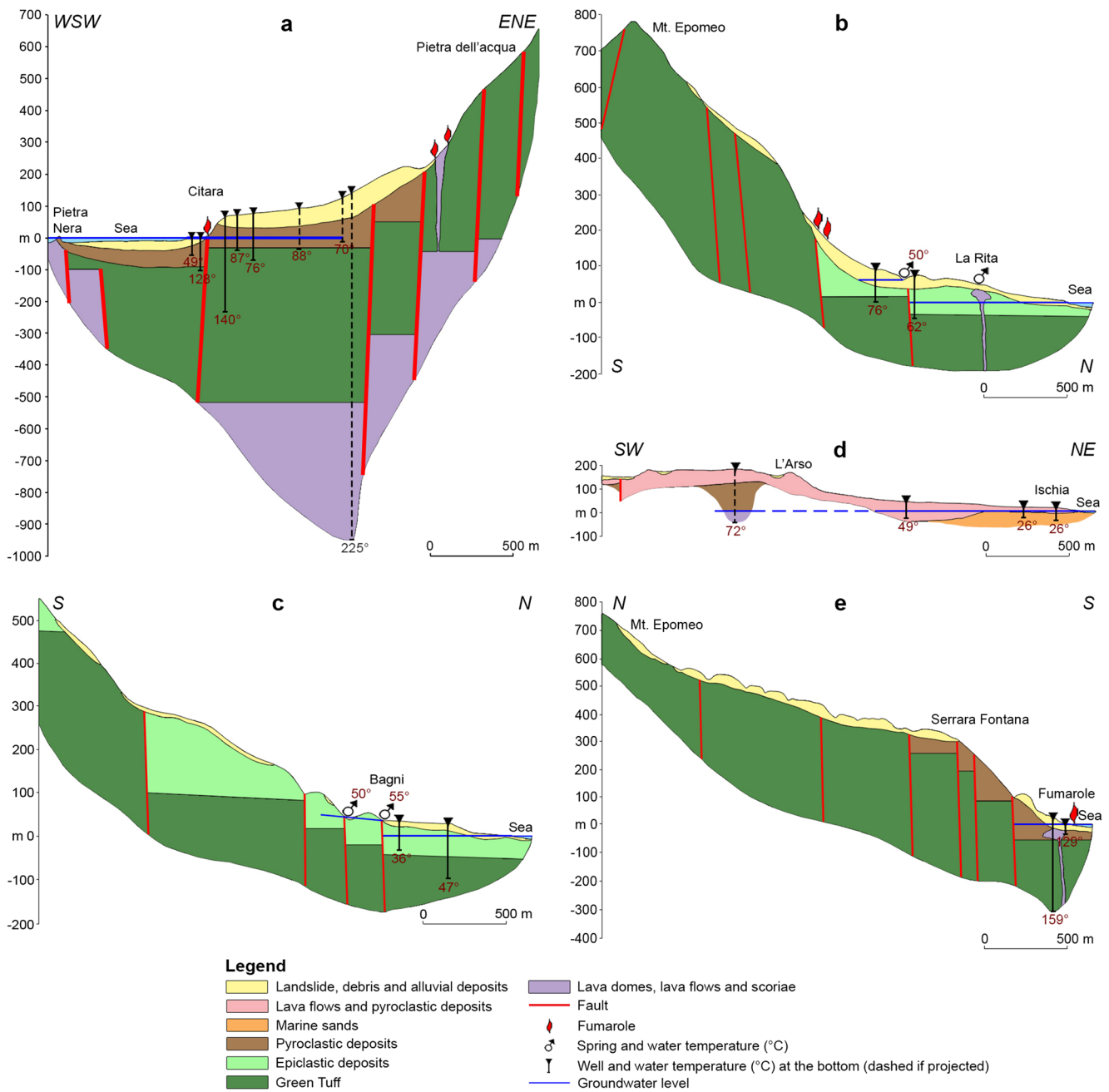
Fig. 4 Hydrogeological cross-sections. **a** Cross-section A–A′, **b** cross-section B–B′, **c** cross-section C–C′, **d** cross-section D–D′, **e** cross-section E–E′ (traces are given in Fig. 2)

Fig. 2). The underlying ignimbrite units correspond to deposits included in the GTA. Through wells of different depth, groundwater flow has been found both in the epiclastic deposits and in the underlying ignimbrite (Fig. 4). However, a lower hydraulic conductivity of the epiclastic deposits compared to the ignimbrite substratum (due to the prevalence of a fine component of the epiclastic layers) allows one to assign a semi-confining role to these deposits with respect to the underlying ignimbrite aquifer formation, which is more intensely fractured.

The PTA groups together pyroclastic fall, surge and flow deposits younger than 55 ka (belonging mainly to Campotese and Fontana-Fasano subsynthems in Fig. 2) and the underlying ignimbrite units, which constitute the aquifer formations in the southern, western and northwestern slopes of Mt. Epomeo (Fig. 3). The pyroclastic deposits mainly include ash, lapilli and breccia tuffs, generally well stratified, from weakly lithified to lithified. These deposits, together with the underlying ignimbrite units (corresponding to deposits included in the GTA),

constitute a continuous aquifer characterized by primary and secondary permeability. In the north-western and southern sector of the island, debris and landslide deposits covering the pyroclastic formations are also part of the aquifer. This is intercepted by wells with different depth, which show a saturated thickness from 0 to 20 m asl to 100 m below it (Fig. 4).

In the south-eastern, south-western and north-western peripheral areas of the island, the PLA includes pyroclastic and lava deposits constituting the aquifer formations (Fig. 3). The pyroclastic deposits are those included in the PTA and GTA, while the lava formations are those constituting the ALA and the younger products. From the few wells available in these areas, the PLA is recognized as an aquifer characterized by a primary and secondary permeability and a variable thickness, with aquifer top at a few meters above sea level and aquifer base up to a few hundred meters of depth.

The VEA includes volcanic, epiclastic and marine deposits younger than 15 ka (belonging mainly to Ischia Porto and La Rita-Caccaviello subsynthems in Fig. 2) constituting the aquifer formations in the north-eastern graben of Ischia (Fig. 3). In the area closest to the coast, the aquifer intercepted by the numerous wells consists mainly of marine sands. Moving towards the interior of the island, the well screens of the few surveyed wells also intercept the pyroclastic and effusive products of the most recent volcanic activity (<15 ka), and the pre-15 ka pyroclastic, epiclastic and effusive units in the southern sector (Fig. 4). The aquifer of the graben of Ischia is to be considered the most permeable of the island in relation to the prevalence of youngest deposits (Celico et al. 1999), that are loose or weakly lithified (with the only exception of the innermost area). Despite the extreme heterogeneity of the volcanic and volcanoclastic products filling the graben of Ischia, a continuous groundwater flow has been recognized with a water level from 0 to 10 m asl, moving from the coastline inward (Fig. 4).

The faults bordering the resurgent block of Mt. Epomeo can play the role of low-permeability barriers due to the strong hydrothermal alteration that characterizes them. This role was inferred by Chiodini et al. (2004) for the faults of the western edge of Mt. Epomeo, where a high soil CO_2 flux has been measured close to an important fumarole field (Fig. 2). The same degree of hydrothermal alteration, and therefore the same hydrogeological role, can be conjectured for the other main faults that border the resurgent block of Mt. Epomeo, if the available maps of fumaroles and radon anomalies (Vezzoli 1988; Molin et al. 2003) are coupled. Conversely, the other minor faults and fractures of Mt. Epomeo and the eruptive fissures of the more recent volcanic activity can be considered more permeable discontinuities.

Springs

An inventory of springs was carried out in the field, starting from information reported in previous studies (Celico et al. 1999; Regione Campania 2008; Di Napoli et al. 2009). Some information includes only the location of the springs and chemical analysis of their waters; most of the "springs" reported in the literature are actually shallow wells. The few spring flow data available in the literature have been supplemented by measures taken in 2014 and 2018.

The results of the inventory of the springs recognized in the island are summarized in Table 1. Seventeen perennial springs (or group of springs) emerge at different elevations, from sea level to approximately 450 m asl (Fig. 2). They differ in flow rate, water chemistry and outcropping conditions. Elevation and flow were determined during the investigations while temperature and salinity were acquired from the literature.

Five springs (1–4 and 14 in Table 1 and Fig. 2) are related to discontinuous perched aquifers of limited extension, presenting one or more of the following features: (1) the springs emerge at the limits between formations with different hydraulic conductivity or within the debris covering the steep slopes of Mt. Epomeo; (2) the flow rate is maximum a few liters per second; (3) the low salinity and temperature of the water, and alkaline bicarbonate or alkaline earth bicarbonate facies correspond with relatively superficial and fast circuits of groundwater. The springs Buceto (1 in Table 1 and Fig. 2) and Nitrodi (2 in Table 1 and Fig. 2) are significant opposite cases. The first one discharges the colder and less mineralized waters of the island and is located at the highest elevation; it can be considered the meteoric water end-member. The spring Buceto emerges at the boundary between the youngest pyroclastic deposits covering the lava dome of Mt. Tripodi (<1 ka) and the epiclastic deposits of Buceto Synthem. Nitrodi spring emerges in the southern slope of Mt. Epomeo, where the recent debris flow and mudflow deposits cover the older pyroclastic and tuff formations; the spring is located at the boundary between clast-supported debris flow deposits and matrix-rich indurated mudflow deposits. The relative high flow of the Nitrodi spring (when compared with other springs of perched aquifers) is due to a large outcrop of debris deposits in its recharge area. The relative high water temperature (28 °C) and salinity (1.2 g/L) of this perched spring can be explained taking into account that it is located at a lower elevation in an intensely fractured sector of the island affected by a high heat flow.

In addition to the inventoried ones, other springs attributable to perched aquifers emerge along the steep slopes of the central sector of the island. Most of them are ephemeral, cold freshwater springs with maximum flow rates less than 0.1 L/s. Eight of the inventoried springs (8–13 and 16–17 in Table 1 and Fig. 2) emerge along the coast at elevations close to sea level. These springs have a flow rate between 0.1 and 2 L/s.

Table 1 Main data of springs (*n.a.* not available)

ID	Spring or group of springs	Elevation (m asl)	Flow (L/s)	Temperature (°C)	Salinity (g/L)	Type of aquifer
1	Buceto	453	< 1	13–18	0.76	Perched
2	Ciglio–La Cesa	250	< 1	18	1.45	Perched
3	Nitrodi	205	3	28–29	1.19–1.29	Perched
4	Olmitello	15	1	26	1.84	Perched
5	Cava Scura	42	2	56–74	5.49–5.78	Basal
6	La Rita	55	2	51–62	4.03–4.42	Basal
7	Piazza Bagni	30–44	15	53–60	3.70–3.71	Basal
8	St. Restituta	1	< 1	34–55	n.a.	Basal
9	San Montano	0	< 1	40–45	n.a.	Basal
10	Castiglione-Bagnitiello	0–2	< 1	30–40	n.a.	Basal
11	Felix	2	2	38	4.19	Basal
12	Terme Comunali	0	2	40	6.00	Basal
13	Cartaromana	0	< 1	32	*na*	Basal
14	Piellero	85	< 1	21	1.61	Perched
15	Castaldi	75	*na*	50	*na*	Basal
16	Sorgeto	0	< 1	82	14.74	Basal
17	Cava Isola	0	< 1	97	23.19	Basal

They emerge at an elevation consistent with the basal piezo-metric head, where the volcanic and pyroclastic formations are locally confined by low-permeability, recent alluvial deposits. Temperature, salinity and chemical composition of the spring waters are similar to those sampled from wells along the coast (Di Napoli et al. 2009). Other springs of the same type are reported in the studies of the 1940s and 1950s, but these springs were not found during the surveys, perhaps because of the significant growth of pumping over time.

Other springs of hydrogeological significance are located in the northern sector of the island at elevations from 30 to 55 m asl (La Rita and Piazza Bagni spring groups, 6 and 7 in Table 1 and Fig. 2). The springs emerge from the fractured epiclastic tuffs (Buceto Synthem) and its debris covering, close to the ENE–WSW to E–W-oriented marginal faults of the resurgent block with the highest displacement of Mt. Epomeo (Fig. 3). The total flow of these springs is about 17 L/s; their water is sodium bicarbonate sulfate with temperature between 30 and 60 °C and salinity between 3.7 and 4.5 g/L (Di Napoli et al. 2009). These hydrogeological characteristics suggest that the springs represent the outflow of the basal aquifer of the resurgent block of Mt. Epomeo, raised if compared to the coastal aquifers. In fact, the wells located upstream of the marginal faults have piezometric heads and water chemistry comparable to the springs (even when the wells deepen in the ignimbrite units underlying the epiclastic tuffs; Fig. 4).

A spring pertaining to this type is the Cavascura spring (5 in Table 1 and Fig. 2), emerging in the southern sector of the island at 42 m asl from the debris deposits with a flow rate of about 2 L/s. The spring waters are sodium chloride and have temperature and salinity of 5.4 g/L and 65 °C, respectively. Referring to some chemical indexes (considered significant in the literature for the classification of groundwater of the island; Di Napoli et al. 2009), the waters of the Cavascura spring are characterized by a Na/Cl ratio of 1.50 and $\delta^{18}O$ of −5.67. These values are intermediate between those of the Buceto spring (Na/Cl = 1.75 and $\delta^{18}O$ = −6.67), representative of a meteoric end-member, and those of the La Rita-Piazza Bagni spring group (Na/Cl = 3.51 and $\delta^{18}O$ = −5.19), representative of the basal aquifer of the resurgent block of Mt. Epomeo. Moreover, the spring that emerges in the western sector from the resurgent block of Mt. Epomeo (15 in Table 1 and Fig. 2) may be due to the outflow of the basal aquifer of the resurgent block of Mt. Epomeo.

Wells

Until 1930, only a limited number of wells were active on the island, being the spas mainly fed by springs (Monti 2004). From 1939 to 1954, 90 wells were drilled for geothermal research, most of them were located in the southern and western coastal areas with depths of a few tens of meters. Only eight wells (Fig. 3) were drilled at depths greater than 100 m (to a maximum of 1,156 m). The results of these investigations were widely examined by several authors (Carlino et al. 2012, 2014).

Since the 1950s, numerous wells have been drilled, mainly to support the activities of the spas and secondly for domestic use. From the analysis of the public bodies' archives (Regione

Campania, unpublished reports 2007 and 2015), research carried out in the past (Celico et al. 1999; Baiocchi et al. 2017) and direct census, approximately 350 wells have been counted on the island (some of these have been abandoned in time, while others correspond to springs). The points do not present the same degree of information, and in many cases only a rough location is known.

The inventoried wells are unevenly distributed in the marginal area of Mt. Epomeo at elevations ranging from sea level to 200 m asl. The highest densities are found where landforms gently connect the beach with the innermost areas of the island, i.e., in the northern, north-eastern, southern and western coastal zones (Fig. 5). The depth, known for 195 wells, varies from 3 m to a maximum of 250 m (Fig. 6; Table 2), with the 75th percentile less than 100 m depth. For 94 wells, water level measurements were carried out at different times (mainly from 1996 to 2017) and well depths and stratigraphy are available; assuming the model is of an unconfined aquifer, the thickness of the saturated zone of the aquifer was computed. It ranges between 2 and 150 m with the 75th percentile less than 50 m thickness (Fig. 6; Table 2). The discharge rate is

available for 133 wells with values varying between 0.2 and 10 L/s (Fig. 6; Table 2), the discharge rate is mostly less than 5 L/s.

The specific capacity of the wells tapping the basal aquifer, derived from the results of 154 step-drawdown tests, is between 8×10^{-6} and 7×10^{-2} m^2/s (Fig. 6; Table 2). No correlation was found between specific capacity and saturated thickness intercepted by the well. The specific capacity has a distribution consistent with the different aquifer formations distinguished on the island: the highest values (generally greater than 1×10^{-3} m^2/s) characterize the younger deposits constituting the aquifer in the north-eastern graben of Ischia (VEA); intermediate values are typical of the pyroclastic and tuff deposits constituting the aquifer in the northern, western and southern marginal zones of Mt. Epomeo (PTA); and the lowest values (generally less than 1×10^{-3} m^2/s) concern the GTA and ETA aquifer formations at the northern and southern slopes of Mt. Epomeo.

Among the historical series of piezometric levels measured every 3 days between the 1930s and 1950s, the most reliable and significant data for the basal aquifer are related to five
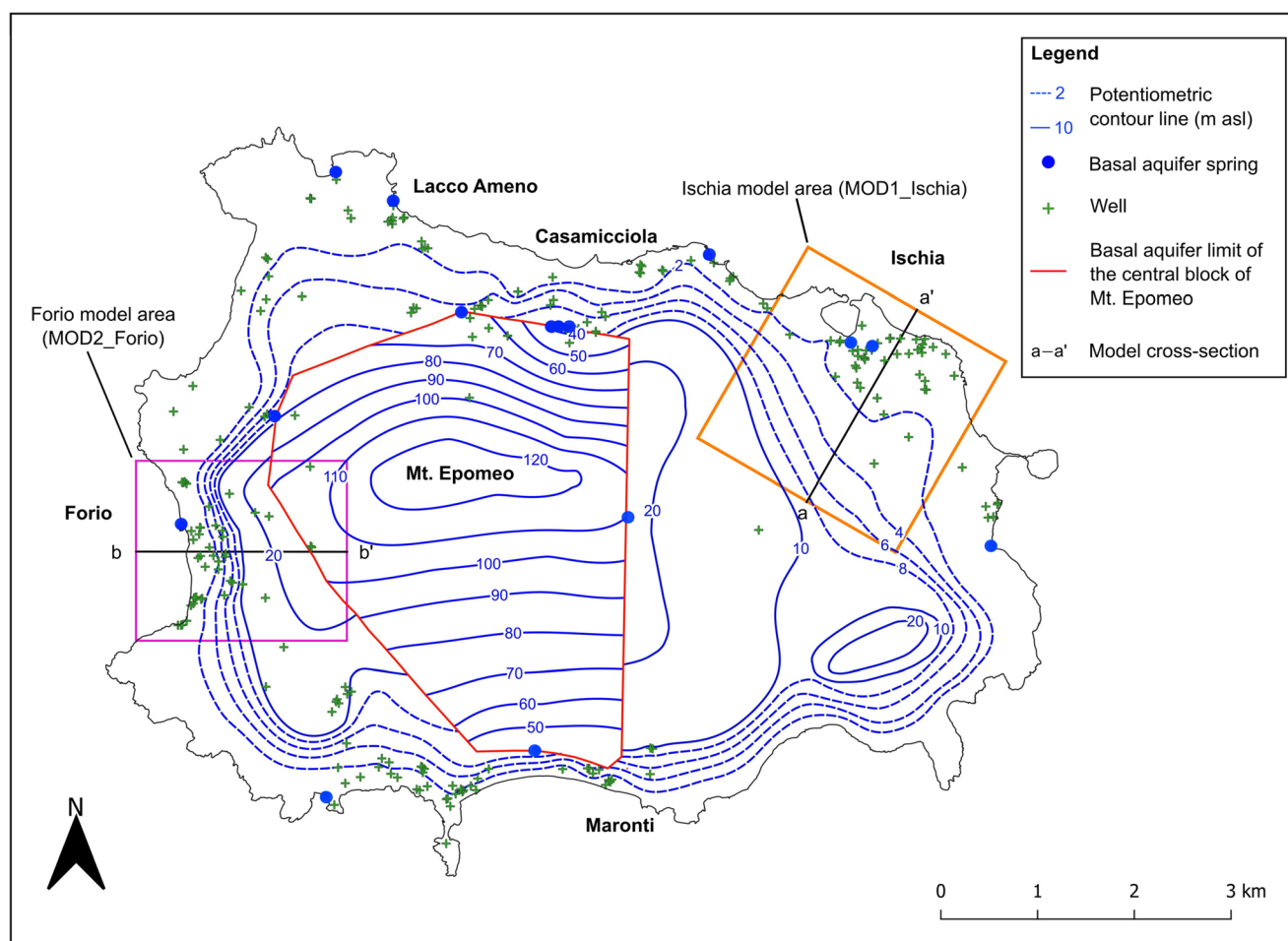

Fig. 5 Potential potentiometric surface of the basal aquifer under static conditions
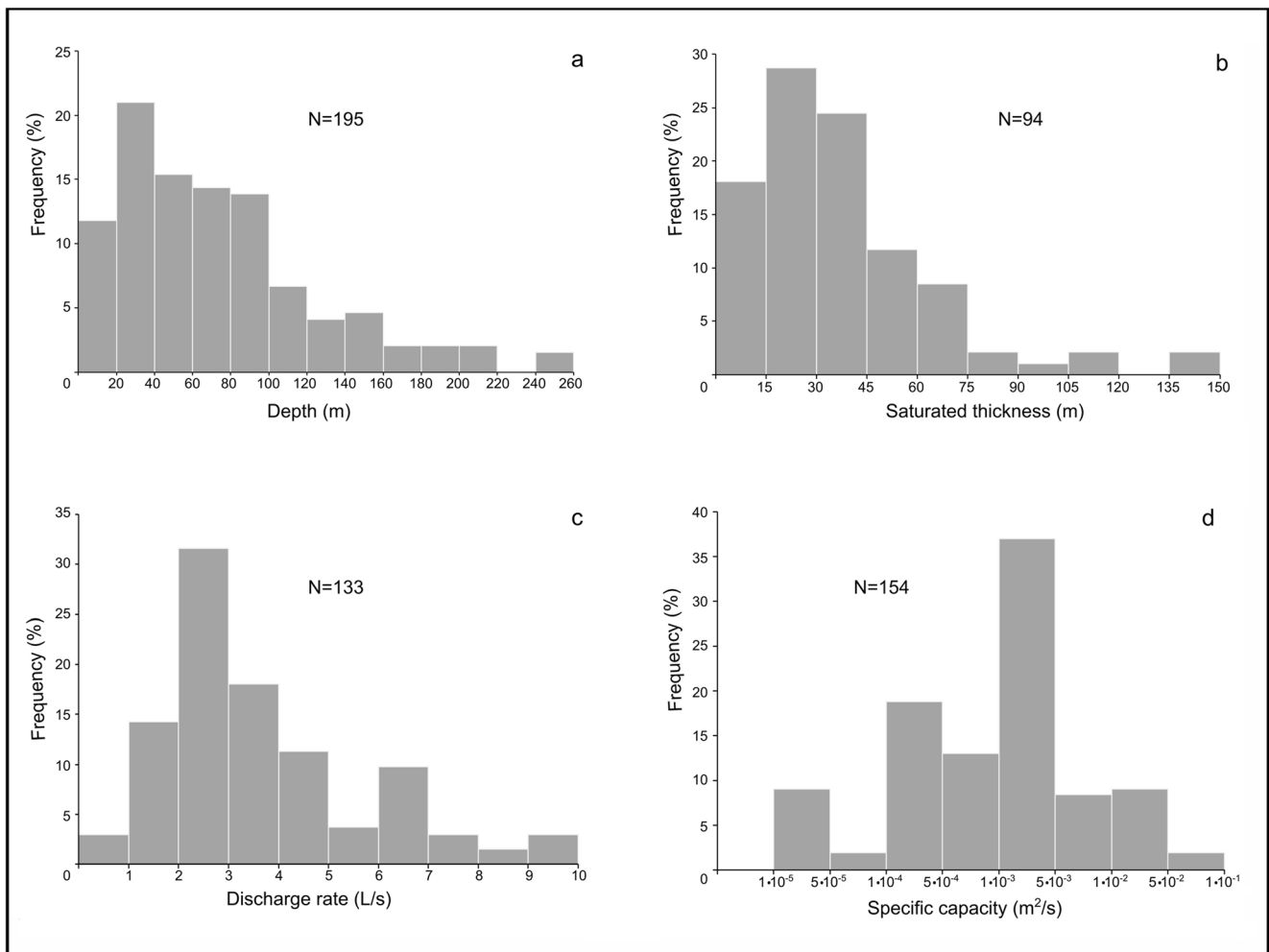
Fig. 6 **a** Frequency distribution of well depth, **b** saturated thickness intercepted by wells, **c** discharge rate and **d** specific capacity of wells

wells located between the coastline and 1.2 km inland in the north-eastern, northern and western sectors (wells 1–5 in Fig. 3). Piezometric head increases from a few decimeters to several meters moving from the coastline towards inland. In the same direction, the annual water-level fluctuation increases from a few centimeters to a few meters. A mean

Table 2 Statistical descriptors of the frequency distributions in Fig. 6. SD standard deviation

Statistical descriptor	Depth (m)	Saturated thickness (m)	Discharge rate (L/s)	Specific capacity (m²/s)
Number (N)	195	94	133	154
Min	2.5	1.5	0.13	8×10^{-6}
Max	250	146.88	10	6.7×10^{-2}
Mean	75.40	37.22	3.73	4.5×10^{-3}
Variance	2880.19	768.31	4.41	1.1×10^{-4}
SD	53.66	27.71	2.10	1×10^{-2}
Median	67.65	30.9	3.16	1.2×10^{-3}
25th percentile	36	17.23	2.23	3.1×10^{-4}
75th percentile	96.75	47.96	4.77	3×10^{-3}
Skewness	1.14	1.75	1.09	4.42
Kurtosis	1.02	3.91	0.87	21.33
Geom. mean	56.33	28.38	3.17	1×10^{-3}
Coeff. Var.	71.16	74.45	56.20	233.03

annual water-level fluctuation of approximately 1 m was obtained from these data.

A comparison of the most complete water-level time series with those for precipitation (1951–1957) highlights the direct influence of rainfall. Cross-correlation results show the maximum correlation coefficient for the first time lag (30–50 days). In the same period, the data of four wells (wells 1, 2, 4 and 5, see Fig. 3) are suitable for recession curve analysis. The values measured during the recession period are interpolated by a negative exponential relationship ($h_t = h_0^{-\alpha t}$, where h_0 is piezometric level at the beginning of the recession period, h_t is piezometric level at time t, and α is the recession coefficient) with a high correlation coefficient ($R^2 > 0.80$). The recession coefficient and depletion period determined for the different years and the different wells range between 7×10^{-4} and 2×10^{-3} day^{-1} and between 160 and 250 days, respectively.

Only one reconstruction of the potentiometric surface of the island is available in the literature (Celico et al. 1999). It considered measurements of 100 wells under static conditions (i.e., without the influence of the pumping) in the period January–March 1996 and covers a large part of the areas located at the edge of Mt. Epomeo.

Many other piezometric levels measured under static conditions were acquired from the archives of public bodies, from previous studies and technical reports, and from recent surveys. On the basis of these data, mainly measured from 1996 to 2017, a new potentiometric surface of the basal aquifer was built in order to cover the whole island (Fig. 5).

Piezometric heads were preliminarily distinguished between basal and perched aquifers considering the well depths, aquifer formations, structural setting, and the distribution and elevation of the springs. Two main areas of the island were recognized: the central sector corresponding with the resurgent block of Mt. Epomeo and the remaining part of the island. The greatest number of piezometric measurements is available for the peripheral coastal sector, even if some areas are completely without wells, such as the south-east ones. To cover unsampled areas, some reconstructed piezometric heads were added to those available, supposed on the basis of the hydraulic gradient measured in comparable conditions by aquifer formation, and taking into account the boundary conditions and the topography.

For the central area of Mt. Epomeo, the following data and assumptions allowed for generation of the potentiometric surface: (1) the elevation of the springs emerging close to the marginal faults of the resurgent block of Mt. Epomeo, (2) the piezometric head of the few wells that are located upstream of the marginal faults, (3) the hydraulic gradient determined by comparing the elevations of springs with the hydraulic heads of wells in the northern slope of Mt. Epomeo, and (4) assuming no-flow boundaries to the east and west of the resurgent block. This latest assumption is based on: (1) the presence of the most important fumarole fields close to the

faults of the western slope of Mt. Epomeo, which can imply a high degree of hydrothermal alteration of the faulted rocks and therefore a local permeability reduction, and (2) the presence of significant thick and low-permeability epiclastic deposits interposed between the uplifted Green Tuff aquifer (GTA) and the shallower volcanic and epiclastic aquifer of Ischia graben (VEA).

The generated map is shown in Fig. 5. The potentiometric surface of the basal aquifer follows the topography, highlighting a radial, divergent flow from the central zone of Mt. Epomeo towards the coastline. The hydraulic gradient varies from a minimum of 0.16% in the sector of the Ischia graben to a maximum of 4.0% in the other marginal sectors of Mt. Epomeo. The highest hydraulic gradient of the island is supposed in the resurgent block of Mt. Epomeo (from 2.5 to 5.5%). At its northern and southern margins, in addition to the groundwater outflows of the basal aquifer through the springs, groundwater flows can occur from the uplifted basal aquifer of Mt. Epomeo towards the aquifer of the coastal sectors with high head losses at the bordering faults.

Main chemico-physical characteristics of groundwater and their relations with the hydrogeology

Through temperature measurements carried out in the deep wells (Fig. 3) drilled in the past in the southern and western areas of the island (up to 1,156 m depth), a geothermal gradient ranging from 0.15 to 0.25 °C/m was determined (AGIP 1987; Carlino et al. 2014). The temperature-depth curves show a significant increase of temperature up to 150 m depth (from 0.40 to 0.53 °C/m), typical of a conductive system. From 150 to 800 m the geothermal gradient is null; below this depth, the temperature profile has been interpreted again as related to a conductive system (Carlino et al. 2014).

New measurements for a groundwater temperature profile were performed in 19 wells of the basal aquifer (Fig. 3) intercepting a saturated thickness from 15 to 150 m. The wells examined show generally an increase in temperature with depth; for three wells, a constant water temperature was measured. The temperature gradient varies between 0.06 and 0.25 °C/m. The lowest temperatures and gradients were measured in the north-eastern sector close to the coastline; the highest temperatures and gradients were measured in the western, northern and southern sectors, even close to the coastline, and in the north-eastern sector in the innermost zones.

For wells that show an increase in temperature with depth, temperature profiles often show a nonlinear trend. For one well located upstream of the marginal faults of the resurgent block of Mt. Epomeo (Fig. 3b), there is a profile useful to estimate the vertical groundwater velocity, according to the Bredehoeft and Papadopulos solution (Bredehoeft and Papadopulos 1965). On the basis of temperature

measurements taken in the semiconfining layer detected between 160 and 240 m of depth (argillified facies of Green Tuff), and assuming a thermal conductivity of saturated material of 1.5 W/mK (Carlino et al. 2014), a groundwater velocity oriented upwards of 7×10^{-9} m/s results.

Other significant data on the water temperature of aquifers intercepted by spa wells are reported in Celico et al. (1999). During pumping tests lasting a maximum of 6 h, the temperature of the water pumped increased from a few degrees up to 30 °C for wells located in the western, northern and southern sectors, even close to the coastline, and in the north-eastern sector in the innermost zones (Fig. 3). Instead, for all the wells located near the coast in the north-eastern sector and for some wells of the northern and western coastal strip, no increase in temperature resulted; in some cases a decrease in temperature was found instead (Fig. 3d). The greatest increases in temperature during pumping (>15 °C) were measured at the Lacco Ameno, Citara and Maronti sites (Celico et al. 1999), where the highest temperatures of groundwater and in deep geothermal wells were found (Di Napoli et al. 2009; Carlino et al. 2014). In these areas, when the temperature of the pumped water reached values above 70 °C, an increase in the piezometric level was monitored rather than the expected drawdown (Fig. 3a), a clear sign of the deep vapor phase rising inside the borehole (Celico et al. 1999).

In five spa wells of the north-eastern sector located close to the coastline (Fig. 3), the electrical conductivity (EC) of the waters with depth was also measured (Fig. 3c). For these wells, characterized by piezometric heads between 0.0 and 0.2 m asl and water temperatures between 21 and 45 °C, the electrical conductivity changed from <10 to >60 mS/cm between 1 and 9 m below the sea level. The sudden change of the parameter can be related to the saltwater intrusion wedge in the sandy deposits which locally constitute the aquifer.

Some chemical parameters of groundwater determined in previous studies were compared with the piezometric head under pumping, as the sampling from wells for the chemical analyses were carried out exactly in these conditions. The Na/Cl ratio and δO^{18} of water are considered by several authors as representative of seawater supply to the aquifer (De Gennaro et al. 1984; Panichi et al. 1992; Di Napoli et al. 2009). Referring to the most recent and complete analytical data reported in Di Napoli et al. (2009), there is a significant correspondence between (1) the coastal areas where the Na/Cl ratio is between 1.0 and 1.5 and the δO^{18} value of water is greater than −2.5, and (2) the coastal strip where piezometric heads under pumping are below sea level. In the north-eastern coastal strip affected by this correspondence, the electrical conductivity logs measured without pumping have shown

that the saltwater intrusion wedge is placed at greater than 1 m below the sea level.

Estimation of meteoric recharge

The recharge by rainfall of the island was estimated on the basis of meteorological data and a preliminary assessment of runoff. The most complete series of precipitation and air temperature data are available for the period 1921–1999 and concern three weather stations of the Italian Hydrographic Service located at an elevation between 8 and 123 m asl (Fig. 7).

The island is characterized by a typical Mediterranean climate with maximum rainfall and minimum air temperature in autumn and winter, and minimum rainfall and maximum air temperature in summer. The average monthly rainfall of the island varies between 9 and 140 mm, while the average monthly temperature is between 9 and 25 °C.

Correlation between elevation and precipitation is not observed in the data set of the Italian Hydrographic Service nor in the less complete data set of Regione Campania (four stations operating for the period 2000–2017 located at elevations between 35 and 370 m asl). The average annual precipitation varies between 851 and 867 mm for the three stations with the most complete series of the Italian Hydrographic Service, and the average value (P) attributable to the island is 860 mm.

Actual evapotranspiration estimation was based on the Turc (1954) method, which is one of the most suitable empirical methods when sufficient climatic data are not available for further processing. In humid regions, this temperature method gives errors similar to other methods such as radiation or combination methods, when compared with lysimeter data (Jensen et al. 1990; Allen et al. 1998). Based on the good inverse linear relationship between the average annual air temperature and elevation in the three stations of the Italian Hydrographic Service ($R^2 = 0.99$), the average annual air temperature could be regionalized as a function of ground elevation. Annual actual evapotranspiration (E) was then evaluated by the constant average annual precipitation of the island and the dependent temperature value from elevation. The values of the parameter range between 388 and 691 mm.

In order to estimate the surface runoff, the geomorphological setting of the island and the results of field surveys were considered. The drainage density varies in the different basins of the island (Fig. 7). The basins with the highest drainage density (from 1.2 to 3.0 km/km^2) are located in the northern and southern slopes of Mt. Epomeo, where a continuous covering of landslide, mudflow and debris deposits outcrops. The drainage pattern of other basins is sparser and tends to disappear in the flat areas; in these basins the surface runoff generated during
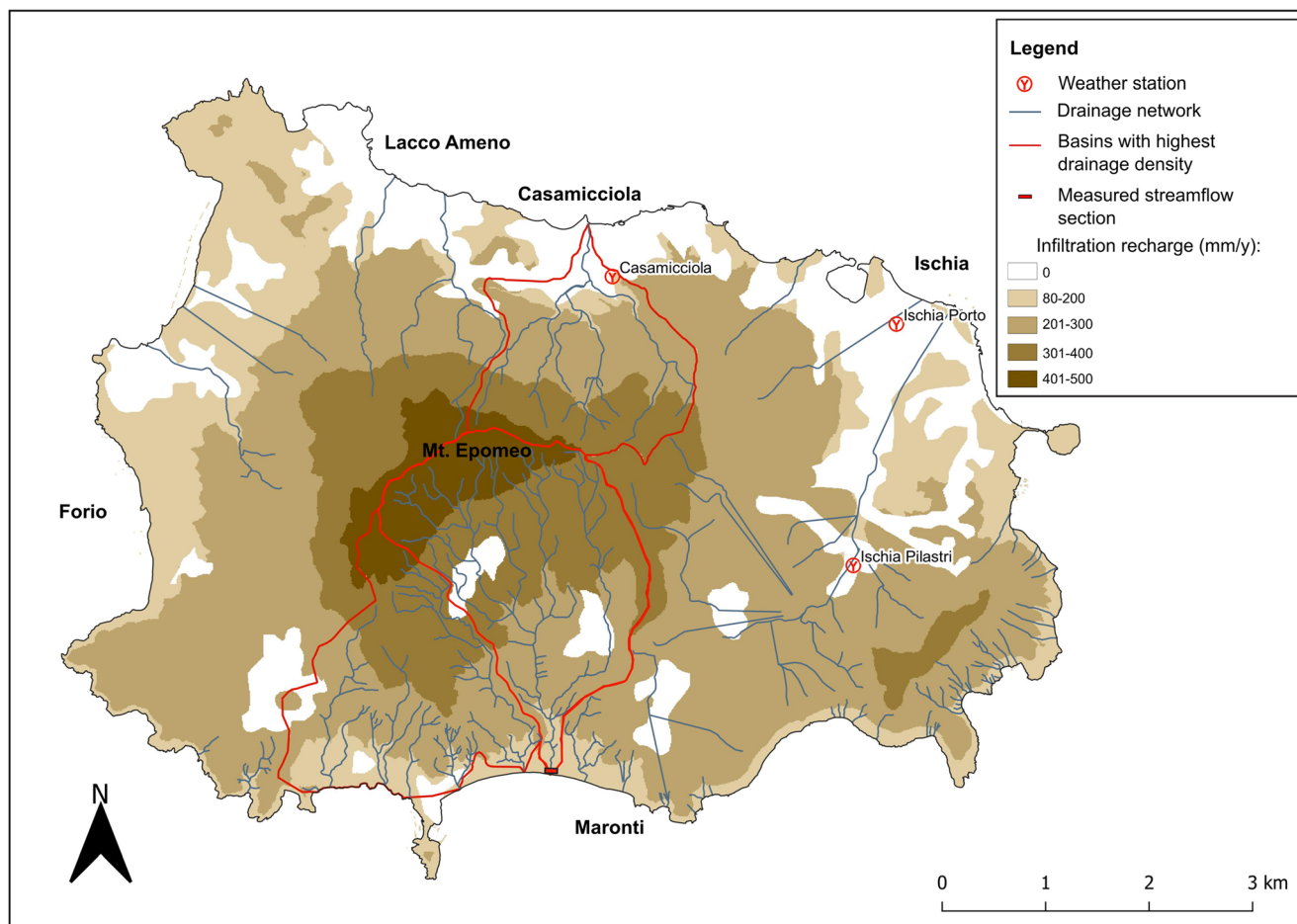
Fig. 7 Distribution of the mean annual rainfall recharge

storm events on steep slopes infiltrates into the stream beds downstream. In the basins of Mt. Epomeo the, streamflow is ephemeral as well only heavy rains generate a significant amount of runoff. The flow rate was measured in a stream draining one of the basins of the southern sector of Mt. Epomeo (Fig. 7) during heavy rainy days in March 2018 with a resulting runoff percentage at 10% of cumulative precipitation.

The rainfall recharge estimate (I) was then obtained considering the land use of the island. Excluding urban areas, the parameter I has been set using $I = P - E$ for the basins with no outflow to sea, and $I = P - E - 0.1 P$ for the basins of the northern and southern slopes of Mt. Epomeo with drainage density greater than 1.2 km/km^2 (Fig. 7). The spatial distribution of the mean annual rainfall recharge is reported in Fig. 7. A recharge of approximately 193 mm/year (equivalent to 284 L/s) results, which corresponds to 6.1 L/s/km^2, in terms of average yield in groundwater of the entire island. This estimate falls within the range of groundwater yield values determined for other volcanic systems of central and southern Italy (Baiocchi et al. 2017 and the literature cited therein) and is about 10% higher than the one determined in previous studies for the island (Celico et al. 1999).

Discussion on conceptual hydrogeological model

New collected data and review of those available, analyzed taking into account the evolution of knowledge on the geological structure, geochemical and hydrothermal models, allow for an update of the conceptual hydrogeological model of the island. The focus was put on the aquifers of the island constituting the first 200 m depth. These aquifers are affected by groundwater withdrawals used for therapeutic purposes and thermal baths.

The decrease in hydraulic conductivity with depth expected especially in the oldest volcanic products, the absence of a relationship between specific capacity of wells and the relative intercepted saturated thickness, the temperature values found in the deep boreholes, the presence of a deep geothermal vapor-dominated system, and the deep vapor phase found to be rising in some shallow wells during pumping, allow for inference of the thickness of the most active groundwater flow. The coastal sector presents the most active layer at a maximum depth of about 100 m below sea level. In the resurgent block of Mt. Epomeo sector, the sea-level elevation can be assumed as a lower limit of the aquifer, due to the expected

decrease in hydraulic conductivity of uplifted ignimbrite formations. Within these depths, groundwater flow assumes specific characteristics depending on the nature of the aquifer formations. In the north-eastern part of the island, where the most recent deposits with the higher permeability prevail, the most active groundwater flows occur in a single and continuous basal aquifer, unconfined or locally semiconfined (Fig. 4). In the northern, western and southern bordering sectors of Mt. Epomeo, in relation to the prevalence of tuffs, ignimbrites and epiclastic deposits, groundwater flow takes place in a continuous basal (confined or semiconfined) aquifer with a general lower permeability (Fig. 4), and locally in overlying, discontinuous perched aquifers. In the central block of Mt. Epomeo, the limited hydrogeological data available suggest the presence of a continuous basal aquifer, uplifted in accordance with the resurgent structure, homogeneously constituted by low-permeability ignimbrite formations (Fig. 4); discontinuous perched aquifers are also present in the formations covering the ignimbrites. The marginal faults of the resurgent block of Mt. Epomeo represent elements of partial discontinuity between the groundwater flow inside and outside the block, as highlighted by the distribution of the springs to their limits and the piezometric heads upstream and downstream of the faults (Figs. 3 and 4). An anisotropic hydraulic conductivity is to be expected in these faulted zones with a vertical component prevailing over the horizontal one.

Based on the reconstructed aquifer geometry, the potential potentiometric surface of the basal aquifer was built in conditions not influenced by pumping (Fig. 5), referring to piezometric data that are temporally and spatially not homogeneous, integrated by a hypothesis about hydraulic heads in areas without wells. Accounting for the aforementioned limitations, the map represents a picture of a possible groundwater flow of the island. It corresponds to a radial flow of the basal aquifer with a zone of high piezometric head in the resurgent block of Mt. Epomeo, which presents groundwater outflows towards peripheral sectors controlled by high head losses through the marginal faults. This conceptual hydrogeological model is consistent with the chemical and isotopic characteristics of the groundwater. For instance, the occurrence of an independent groundwater flow in the block of Mt. Epomeo agrees with some significant geochemical indicators of the waters of the springs and wells falling at the edges and inside it, respectively. Temperature, salinity, Na/Cl ratio and δO^{18} of these waters are intermediate between those characterizing the freshwater of perched aquifers (Buceto spring) and those related to the basal aquifer of the marginal sectors of the island.

The most significant effect of pumping from wells is the lowering of the piezometric level below sea level in the coastal zones, where there is the greatest density of spa wells. These piezometric conditions explain the high salinity, the lower values of δO^{18} and the Na/Cl ratio close to 1 of the waters sampled from the wells of the coastal zones (Di Napoli et al.

2009). In other words, during the pumping period, the seawater wedge advances in the innermost areas of the island. The seawater intrusion is more severe in the northeastern coastal zone, due to the large number of wells and the high hydraulic conductivity of the aquifer, and in the western coastal area, mainly due to the very high density of wells. In the other coastal zones, the seawater intrusion is more contained due to a lower density of pumping wells and a lower hydraulic conductivity of the aquifer. During the pumping period, the basal aquifer is recharged by the seawater, in addition to rainfall and deep fluids.

Referring to the previous estimate (Celico et al. 1999) and the one conducted in this study, the meteoric recharge is between 257 and 284 L/s. Comparing these rates with the mean annual water-level fluctuation of the island (approximately 1 m), average values of the specific yield between 0.18 and 0.19 result. These values are consistent with the ones known in the literature for the rocks constituting the aquifer (Domenico and Schwartz 1997).

The bottom recharge of the aquifer can be roughly estimated considering the vertical groundwater velocity (7×10^{-9} m/s), calculated from the temperature profile measured upstream of the marginal faults of the block of Mt. Epomeo (Fig. 3b). This value can only be attributed to the aquifer sector where a semi-confining layer is clearly recognizable and where a similar water temperature profile with depth is to be expected, that is the area of the resurgent block of Mt. Epomeo. Under these assumptions, approximately 90 L/s of recharge from the bottom of the aquifer results. This rate is to be considered as a minimum value, because there are insufficient data to determine the vertical groundwater velocity in the other sectors of the island characterized by the increase in water temperature with depth. It is also necessary to consider the possible deep-fluid rises through the marginal faults of Mt. Epomeo, as deduced from the geochemical and hydrothermal models. As it often happens, a direct estimate on the basis of the available data is rather complex. According to Di Napoli et al. (2009), a rate of about 50 L/s of magmatic water could supply the hydrothermal system of the island.

Therefore, under undisturbed conditions (i.e., without pumping from the aquifer), an average meteoric recharge equivalent to a flow of about 250–290 L/s and a recharge from the bottom equivalent to at least 90 L/s are to be considered for the aquifer of the island. When the wells are actively pumping, a further recharge from seawater must be considered.

A rough estimate of what happens in the period of simultaneous pumping from all the wells can be obtained by the relationship of Pinder and Jones (1969): $C_w Q_w = C_s Q_s + C_a Q_a$, where C_w and Q_w are the water chloride concentration and the flow rate of the wells located in the coastal zone, respectively; C_s and Q_s are the chloride concentration and component of the flow rate of seawater in pumped water, respectively; C_a and Q_a are the chloride concentration and the

component of the flow rate of groundwater not influenced by seawater intrusion in pumped water, respectively. Considering that $Q_w = Q_s + Q_a$ is equal to approximately 300 L/s (i.e., the total flow from wells in the peak tourist season), and assuming C_s is equal to 650 meq/L, and for C_w and C_a the average concentrations from chemical analyses are 300 and 20 meq/L, respectively, approximately 44% of the total flow pumped from the wells in the coastal zone derives from seawater.

Possible impacts of withdrawals of thermal waters

The review of the conceptual model shows that the assessment of the impacts of groundwater withdrawals on the island is complicated by the interactions of fluids with different origins and composition (meteoric recharge, deep fluids and seawater) in heterogeneous aquifers. The sustainability of groundwater withdrawals is essentially related to maintaining the quality of the water pumped by the numerous wells. The quantity of groundwater resources tapped from the wells does not seem to be a reliable indicator of sustainability, since the wells pumped along the coast are recharged from seawater and the innermost wells are recharged from deep fluids. However, both the contributions of seawater and deep fluids can have effects on the quality of the water pumped from the wells that feed the spas such as changes over time in temperature and chemical composition. This can represent a problem, since the Italian legislation establishes that composition and temperature of mineral and thermal waters must remain constant as much as possible (Italian Legislative Decree 176/2011 implementing UE Directive 2009/54/CE).

To examine the possible impacts of the withdrawals on the quality of the thermal waters, two approaches were used: the analysis of the relationships between amount of withdrawals and quality of the pumped water, and simplified numerical investigations.

Approaches

The amount of withdrawal from wells was estimated using the data acquired from the public data base, unpublished reports and the inventory of wells conducted during the investigations. Information on the variation in the quality of water pumped from wells was derived from previous geochemical surveys (Di Napoli et al. 2009) and unpublished reports from the Campania Region. The temperature logs under static conditions, water temperature during pumping, drawdown and flow rate measured during the investigations (Fig. 3) were also analyzed.

At the current state of knowledge, numerical models of density-dependent flow and heat transport are difficult to set up and calibrate, due to the complexity of the conceptual

model, an incomplete characterization of the parameters and boundary conditions of the system, and above all a lack of useful data for history matching. Simplified numerical models were built, reproducing the basic features of the two areas with the highest number of wells (Fig. 5). The approach consisted in assigning zones of constant hydrogeological parameters over the model domain, regardless of the high heterogeneity of the area, impossible to estimate given the poor quality of the present datasets. Finite difference models were built using MODFLOW-2005 (Harbaugh 2005) and SEAWAT (Langevin et al. 2003); the codes were applied through the graphic user interface Groundwater Vistas 7 (Rumbaugh and Rumbaugh 2017). For the reconstruction of the surfaces, the top of the first layer was extracted by the digital elevation model, while the other surfaces were based on the hydrogeological cross-sections (Fig. 4) or arbitrarily assigned.

The modeling process included two steps. In the first step, groundwater flow was modeled considering the specific hydrostratigraphic structure and boundary conditions, and assigning hydraulic conductivity values included in the local reliable ranges. Time was discretized into two steady-state stress periods: the first one representing the natural conditions without pumping and the second representing the aquifer under pumping. The potentiometric surface resulting from the model for both the first and second stress periods could be only qualitatively compared with those known from the measured data, given the high noise present in measurements.

In a second step, groundwater flow coupled with solute transport was simulated through SEAWAT. In this case, the transport process was divided into two transient stress periods. The first stress period lasted 250 years, to allow the seawater interface to reach the natural equilibrium. The second stress period lasted 25 years, simulating a continuous pumping from the wells equivalent to the period of about 50 years in which the wells of the spas worked for at least 6 months/year. The distribution of selected chemical indicators resulting at the end of the second stress period was qualitatively compared with the available chemical analyses in the two areas to evaluate the incidence of the different components (meteoric recharge, seawater intrusion and deep fluids) on the water captured from the wells.

Relationships between the amount of withdrawals and the quality of the pumped water

Available data on changes in water composition and temperature over time are scarce and sometimes incongruent. According to the monitoring conducted by Di Napoli et al. (2009) on a dozen thermal waters in the period 2002–2007, a stability of composition results. In particular, a variation of less than 30% of temperature results for most of the monitored points, some more marked variations (up to 40 °C) are explained in relation to changes in use of groundwater and in tapping methods. The authors also observe a

Table 3 Estimates of thermal water withdrawals

Source area	Regione Campania 2015				Present study	
	N well	N spring	Q (L/s)	V (m³/ year × 10⁶)	N well and spring	Q (L/s)
North East	63	0	204	0.288	51	233
West	65	1	169	0.426	47	134
North	62	16	139	0.261	41	87
South	54	3	141	0.239	40	113
Island	244	20	653	1.214	179	567

Q = flow rate, V = withdrawal volume

constant Mg–Cl ratio, interpreted as a constant contribution of deep-rising.

Studies commissioned by the Campania Region have examined the historical trends of some components of groundwater from the 1980s to 2010 (Regione Campania, unpublished reports, 2007 and 2015). These unpublished reports highlight the difficulties in comparing

chemical analyses of different periods, since analytical precision is not always specified, the sampling points are not always fully identified, and flow rate and pumping time of the sampled wells are often unknown. Unique pieces of evidence are an increase over time in chloride concentration and a decrease in temperature of the waters (approximately 5 °C) pumped from the north-eastern coastal area of the island.

The trend over time of the composition and temperature of the thermal waters, however, must be examined taking into account the rate and distribution of the groundwater withdrawals. While the distribution of wells is known, data on the amount of withdrawals are not complete. Table 3 shows the available data for the different hydrogeological areas of the island. The flow rate of the wells (Q) refers to the one used during the period of operation of the spa facilities; however, the period of operation of the wells is not known. The annual withdrawal volumes (V) reported in Table 3 refer to those declared by the concessionaires. In the hypothesis of a tourist season of about 180 days, considering the values of Q and V would result in a period of operation of the wells of about 3 h/

Fig. 8 Relationships between: **a** temperature variation (ΔT) and drawdown (Δh), and **b** temperature variation and specific capacity (Q_s). The circles indicate an increase in temperature, the squares indicate a decrease in temperature

$\Delta T = 1.2136\, \Delta h + 1.8195$
$R^2 = 0.98$

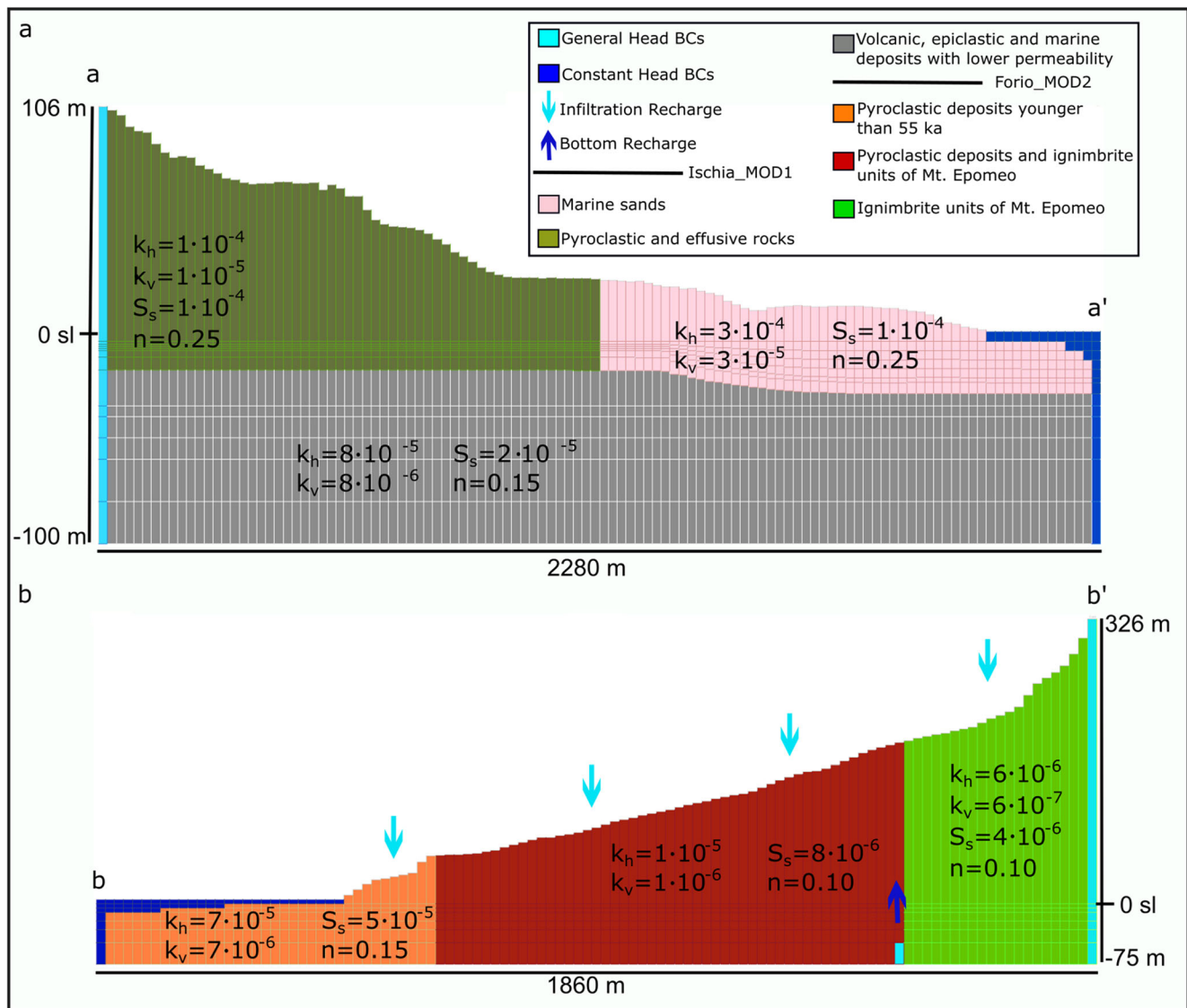$\Delta T = 0.2974\, Q_s^{-0.442}$
$R^2 = 0.82$
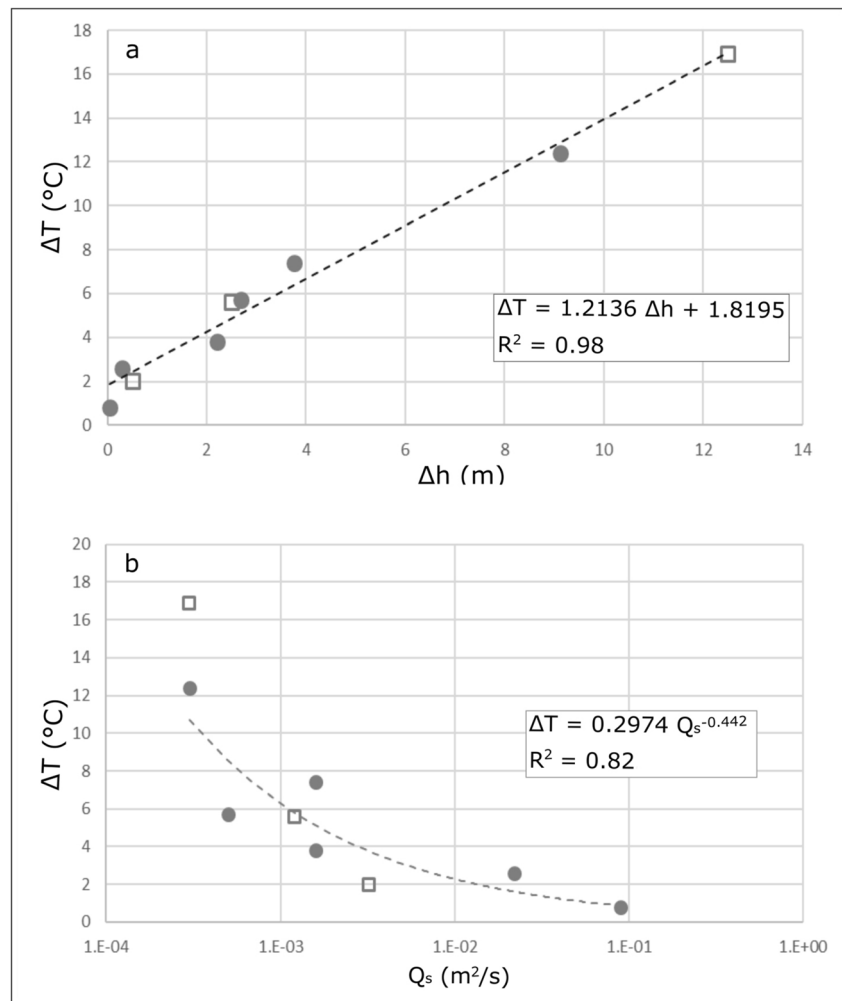
Fig. 9 **a** Cross-sections of the Ischia_MOD1 model and **b** Forio_MOD2 model (traces are given in Fig. 5) showing the boundary conditions and zones with different hydrogeological properties. The values of hydraulic conductivity (horizontal, k_h, and vertical, k_v, in m/s), porosity (n) and specific storage (S_s in m^{-1}) are distributed in simplified uniform zones

day. This estimate appears to be unreliable if, for example, the volume of the operating swimming pools is considered. Instead, the estimate of the flow rate of pumping (Q) may be considered reliable, if data reported by the public bodies and those acquired during investigation are compared.

A total flow between 540 and 620 L/s is then simultaneously pumped during the period of operation of the spa facilities (being approximately 28 L/s derived from the natural flow of the springs). This flow is significantly higher than the estimated average meteoric recharge value (250–290 L/s). Therefore, during the tourist season, a portion of the pumped water is recharged by the deep fluids and seawater, as well as from the aquifer storage. Maintaining the quality of the thermal waters in a narrow natural interval, as established by the legislation, thus

implies that the pumped water is not significantly influenced by one of these components with different temperature and composition. This equilibrium depends on the location and depth of the wells, local aquifer hydraulic diffusivity and heat flow. The measured data from nine wells distributed in the north-eastern and western coastal areas showed what happens during pumping. From the comparison among the water temperature under static conditions, during pumping, drawdown and flow rate, a direct correlation exists between temperature variation and drawdown, and an inverse correlation exists between temperature variation and specific capacity (Fig. 8). The observed increases and decreases in temperature can be interpreted by the influence under pumping of deep fluids and seawater, respectively.
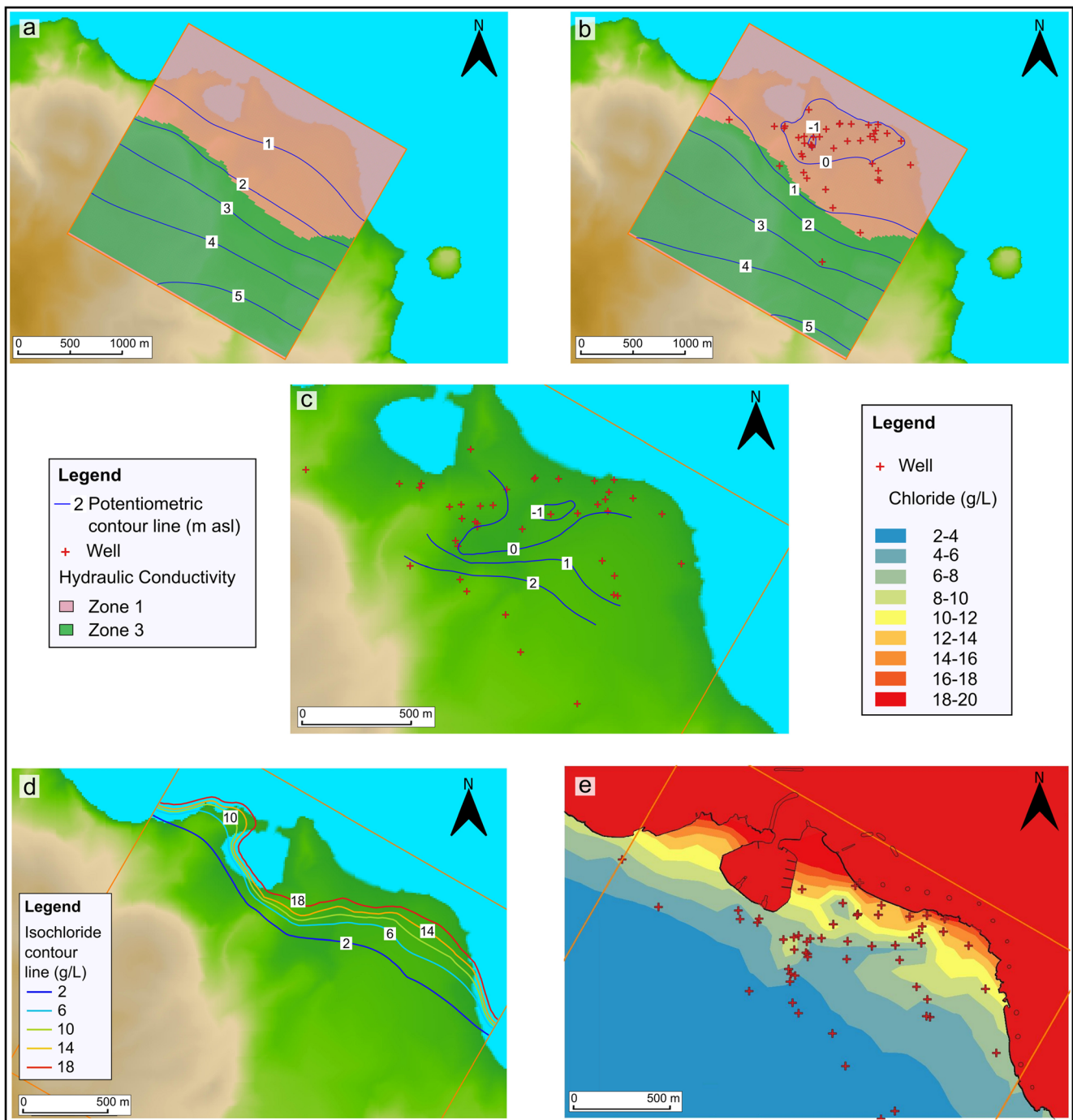
Fig. 10 Results of Ischia_MOD1: **a** simulated potentiometric surface under undisturbed conditions, **b** simulated potentiometric surface under pumping, **c** potentiometric surface under pumping reconstructed from the measured data, **d** simulated distribution of chloride concentration in the third layer, **e** distribution of chloride concentration reconstructed from the chemical analysis of well waters (from Di Napoli et al. 2009)

Results of numerical investigations

The two selected areas, i.e., the north-eastern (Ischia) and western coastal (Forio) areas (Fig. 5), schematize two different hydrogeological settings found in the island, characterized by the highest density of groundwater withdrawal. Model areas cover approximately 5 km^2 in the north-eastern sector of the island (Ischia_MOD1) and 4 km^2 in the western one (Forio_MOD2); these areas were horizontally discretized by grids of 174,876 and 70,959 cells respectively, with a uniform cell size of 20 × 20 m. The vertical discretization includes 13 layers for Ischia_MOD1 and 7 layers for Forio_MOD2 to better reproduce the seawater ingression and the local hydrostratigraphy.

Table 4 Simulated flow (L/s) in Ischia_MOD1

Term	Undisturbed		Under pumping	
	Inflow	Outflow	Inflow	Outflow
Upstream inflow	122.1	–	139.8	–
Inflow from sea	14.4	–	67.2	–
Outflow to sea	–	137.6	–	34.9
Discharge from wells	–	–	–	172.6

Table 5 Simulated flow (L/s) in Forio_MOD2

Term	Undisturbed		Under pumping	
	Inflow	Outflow	Inflow	Outflow
Upstream inflow	21.7	–	34.8	–
Infiltration recharge	20.2	–	20.2	–
Bottom recharge	5.6	–	7.2	–
Inflow from sea	–	–	61.5	–
Outflow to sea	–	47.7	–	–
Discharge from wells	–	–	–	123.8

The boundary conditions included GHB (general head boundaries) to simulate head-dependent lateral inflow from the central part of the island, and CHB (constant head boundaries) to represent the sea outflow/inflow (Fig. 9). Rainfall recharge was considered only in Forio_MOD2, being the area of Ischia_MOD1 largely urbanized. In Forio_MOD2, a bottom recharge of the aquifer was applied as GHB, representing the estimated inflow from the marginal faults of Mt. Epomeo. In each model domain, the wells of the spas were imported with their depths and pumping flow rates: 43 wells in

Ischia_MOD1 for a total discharge of 173 L/s and 35 wells in Forio_MOD2 for a total discharge of 124 L/s.

In Ischia_MOD1, the subsoil up to 100 m below sea level was schematized in three zones with different hydrogeological properties in accordance with the aquifer formation characterization (Fig. 9a): a shallow zone close to the coast where the aquifer formation consists of marine sands, a shallow innermost zone where the aquifer consists of pyroclastic and effusive rocks, and a deeper zone, extended over the whole model
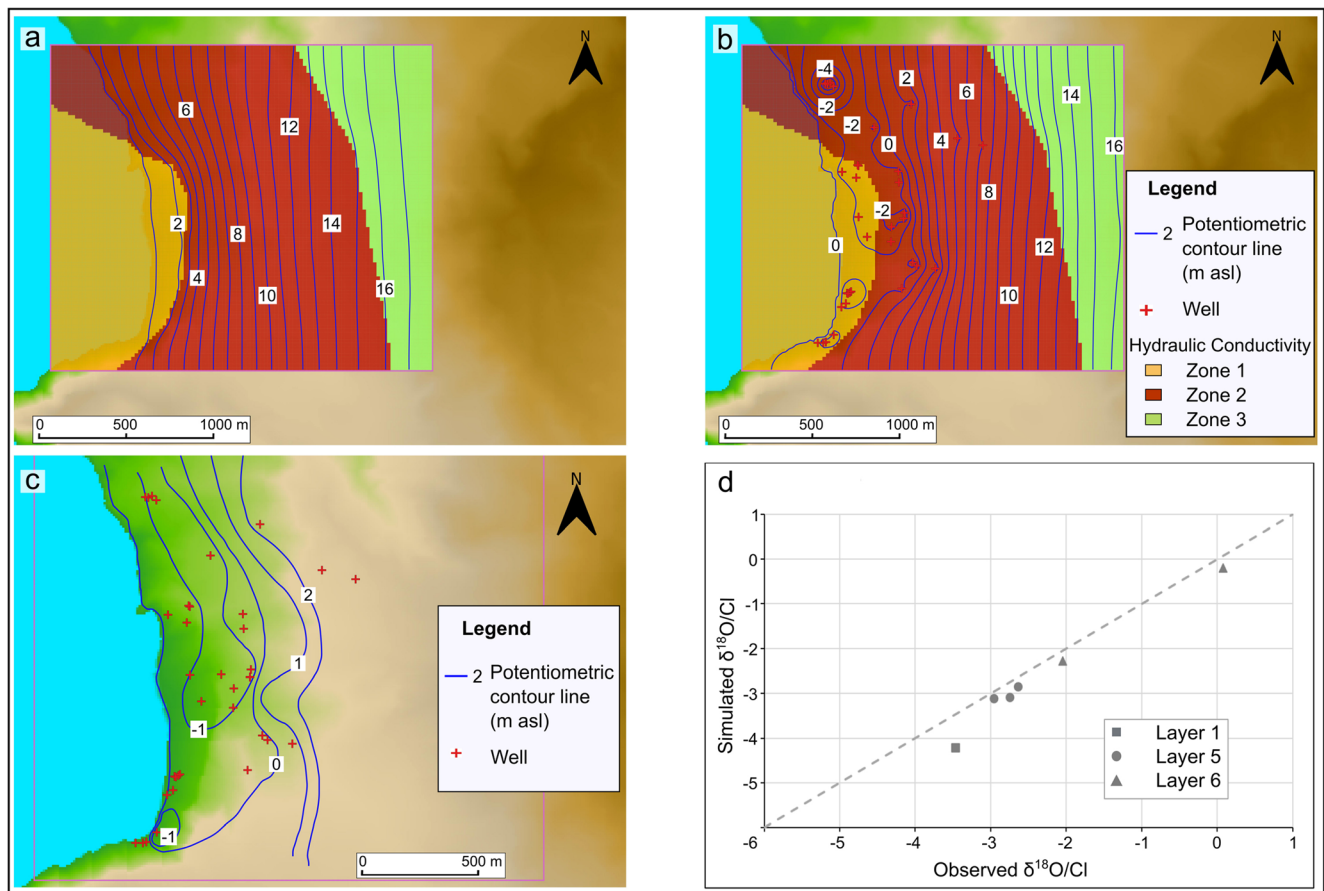

Fig. 11 Results of Forio_MOD2: **a** simulated potentiometric surface under undisturbed conditions, **b** simulated potentiometric surface under pumping, **c** potentiometric surface under pumping reconstructed from the measured data, **d** scatter plot of simulated vs observed values of $\delta^{18}O/Cl$ ratio (measured values from Di Napoli et al. 2009)

domain, representing the decrease of permeability with depth. In this coastal area, the conceptual model mainly points towards inflow from the upstream boundary and seawater intrusion, therefore the chloride concentrations were used as an indicator to examine the influence of the two components in the waters captured by the wells. The chloride concentrations of the upstream inflow and seawater were set equal to 0.1 and 20 g/L, respectively.

Comparisons between the results of the model and the measured piezometric levels and concentrations of chloride (the latter mainly derived from Di Napoli et al. 2009) are shown in Fig. 10. The flow rates resulting from the model under undisturbed conditions and under pumping are reported in Table 4. On the basis of the results of the model, under the assumed pumping conditions in the north-eastern part of the island, an increase in inflow from the upstream boundary of 14% occurs during the pumping and 19% of the water pumped from the wells derives from seawater.

In Forio_MOD2, the subsoil up to 75 m below sea level was schematized in three zones with different hydrogeological properties (Fig. 9b): a zone close to the coast where the aquifer formation consists of pyroclastic deposits younger than 55 ka, an intermediate zone where the aquifer is formed by the aforementioned pyroclastic deposits and underlying ignimbrite units of Mt. Epomeo, and an innermost zone where the aquifer consists of the Mt. Epomeo ignimbrite units. The rainfall recharge assigned to the model was derived from the distribution of the mean annual rainfall recharge (Fig. 7). The bottom recharge through the faults was calculated on the basis of a hypothesized water pressure at 75 m below sea level (about 10 Pa according to Carlino et al. 2014).

In this coastal area, where the conceptual model highlights interactions among inflow from the upstream boundary, rainfall recharge, seawater intrusion and deep fluids rise, the ratio between $\delta^{18}O$ and chloride concentration was selected as an indicator to examine the influence of the different components in the waters captured by the wells. This choice was based on the results of geochemical models (Di Napoli et al. 2009) and the availability of sufficient chemical data for the specific area. The $\delta^{18}O/Cl$ ratios of the three different end-members, i.e., seawater, meteoric recharge and bottom recharge, were derived from Di Napoli et al. (2009) and set equal to 0.09, −3.72 and −0.89, respectively. The uniform hydrogeological parameters of the three zones were adjusted comparing the available measured piezometric levels, under undisturbed and pumping conditions, and the values of the $\delta^{18}O/Cl$ ratios derived from Di Napoli et al. (2009). Given that the available data on the $\delta^{18}O/Cl$ ratio for this sector of the island are unevenly distributed and the depth of the sampled well is not always known (some of them refer to perched aquifers rather than the basal aquifer), the adjustments tended to follow the general local trend, based only on the wells with known characteristics. The results obtained from the model are shown in

Fig. 11, in terms of potentiometric surface, along with a scatter plot of simulated and observed $\delta^{18}O/Cl$ ratio. The related values of hydrogeological parameters are reported in Fig. 9. The flow rates resulting from the model under undisturbed conditions and under pumping are reported in Table 5. In this case, under the assumed pumping and boundary conditions, increases in inflow from the upstream boundary and from the bottom recharge of 60 and 28% respectively occur during the pumping; moreover, 50% of the water pumped from the wells derives from seawater.

Concluding remarks

In the small volcanic island of Ischia, located in a high heat flux zone (about 500 mW/m^2), the structural setting and the wide variety of stratigraphic units are the key factors affecting groundwater flow in the aquifers constituting the first 200 m of depth.

In the resurgent block of Mt. Epomeo, an independent and uplifted basal groundwater circulation can be inferred by a cross-check of the ignimbrite stratigraphic succession and hydrogeological and hydrogeochemical data of a few wells and springs located at its edge. The marginal faults of the resurgent block constitute the hydrogeological partial barriers to the basal groundwater flow of this part of the island's aquifer; furthermore, they represent the preferential ways of ascending deep fluids.

In the peripheral areas of Mt. Epomeo, groundwater flow is mainly influenced by the nature of the aquifer formations. In the northern, western and southern areas, a continuous basal aquifer and local discontinuous perched aquifers can be distinguished consistently with a succession of tuffs, ignimbrites and epiclastic deposits. In the north-eastern area, characterized by the most recent volcanic deposits of the island, a single and continuous basal aquifer with the highest permeability in the island results. In these peripheral areas of Mt. Epomeo, the flow and the chemical characteristics of the waters of shallow aquifers depend not only on natural phenomena but also on the intensive groundwater abstraction supplying the numerous thermal establishments.

In natural conditions, the hydrogeological system of the island is recharged by rainfall (a total of about 250–290 L/s) and by deep fluids (at least 90 L/s); the discharge is towards the sea and the springs. In the peripheral areas of Mt. Epomeo, when a total discharge of about 600 L/s is pumped during the peak season, a significant additional recharge of the aquifers derives from seawater and from upwelling increase of deep fluids. Although this does not compromise the availability of groundwater in quantitative terms, the pumping modulates the quality of the water captured by the wells.

As a matter of fact, the great variability in the chemical and isotopic composition of groundwater is due not only to the

local hydraulic parameters of the aquifers, but also to the discharge rates, depth and characteristics of wells from which the water is sampled. The mixing between the different end members (meteoric water, seawater and thermal members), as described in the literature, is strongly influenced by the local response of the aquifer to pumping.

The examined case represents an uncommon occurrence among small volcanic islands: the high heat flux and volcanological features of the island affect the quality of groundwater, as well as its main use for the flourishing spa tourism. The geogenic scarcity of drinkable resources and the proximity of the island to the continent allows the importation of water resources for human consumption. This excludes the typical problems affecting the management of water resources of small islands such as saltwater intrusion (UNESCO 1991). On the contrary, in the case of Ischia the interaction among meteoric water, seawater and deep fluids represents a condition of considerable value for the island's economy. However, due to the fragile hydrogeological equilibrium detected by this study, the maintenance of a stable quality of the unique mix of waters found in Ischia, as well as their use for an effective volcanic hazard monitoring, cannot disregard the overall control and regulation of flow rate and duration of pumping in the hydrogeologically different sectors of the island.

References

Acocella V, Funiciello R (1999) The interaction between regional and local tectonics during resurgent doming: the case of the island of Ischia, Italy. J Volcanol Geotherm Res 88:109–123

AGIP (1987) Geologia e geofisica del sistema geotermico Dei Campi Flegrei [Geology and geophysics of the Phlegraean fields geothermal system]. Technical report. Settore Esplorazione e Ricerche Geotermiche, San Donato Milanese, Italy, 23 pp

Aiuppa A, Avino R, Brusca L, Caliro S, Chiodini G, D'Alessandro W, Favara R, Federico C, Ginevra W, Inguaggiato S, Longo M, Pecoraino G, Valenza M (2006) Mineral control of arsenic content in thermal water from volcano-hosted hydrothermal systems: insights from island of Ischia and Phlegrean fields (Campanian Volcanic Province, Italy). Chem Geol 229:313–330

Allen RG, Pereira LS, Raes D, Smith M (1998) Crop evapotranspiration. Irrigation and Drainage Paper no. 56. UN Food and Agriculture Organization, Rome

Baiocchi A, Formica F, Lotti F, Pianese L, Piscopo V, Summa G (2017) Occurrence, management and protection of mineral and thermal waters in some volcanic areas of Italy: current knowledge and future directions. Sustain Water Resour Manag. https://doi.org/10.1007/s40899-017-0132-5

Beccaluva L, Di Girolamo P, Serri G (1991) Petrogenesis and tectonic setting of Roman Volcanic Province, Italy. Lithos 26:191–221

Bredehoeft JD, Papadopulos IS (1965) Rates of vertical groundwater movement estimation from Earth's thermal profile. Water Resour Res 1:325–328

Caliro S, Panichi C, Stanzione D (1999) Variation in the total dissolved carbon isotope composition of thermal waters of the island of Ischia (Italy) and its implications for volcanic surveillance. J Volcanol Geotherm Res 90:219–240

Carapezza M, Hauser S, Parello F, Scelsi E, Valenza M, Favara R, Guerrieri S (1988) Preliminary studies on the geothermal fluids of the island of Ischia: gas geochemistry. Rend Soc Ital Mineral Petrol 43:967–974

Carlino S (2012) The process of resurgence for Ischia Island (southern Italy) since 55 ka: the laccolith model and implications for eruption forecasting. Bull Volcanol 74:947–961

Carlino S, Somma R, Troise C, De Natale G (2012) The geothermal exploration of Campanian volcanoes: historical review and future development. Renew Sust Energ Rev 16:1004–1030

Carlino S, Somma R, Troiano A, Di Giuseppe MG, Troise C, De Natale G (2014) The geothermal system of Ischia Island (southern Italy): critical review and sustainability analysis of geothermal resource for electricity generation. Renew Energy 62:177–196

Celico P, Stanzione D, Esposito L, Formica F, Piscopo V, De Rosa BM (1999) La complessità idrogeologica di un'area vulcanica attiva: l'Isola d'Ischia (Napoli-Campania) [The hydrogeological complexity of an active volcanic area: the island of Ischia (Naples-Campania)]. Boll Soc Geol It 118:485–504

Chiodini G, Avino R, Brombach T, Caliro S, Cardellini C, de Vita S, Frondini F, Granirei D, Marotta E, Ventura G (2004) Fumarolic and diffuse soil degassing west of Mount Epomeo, Ischia, Italy. J Volcanol Geotherm Res 133:291–309

Civetta L, Gallo G, Orsi G (1991) Sr- and Nd-isotope and trace element constraints on the chemical evolution of the magmatic system of Ischia (Italy) in the last 55 ka. J Volcanol Geotherm Res 46:213–230

Crisci GM, De Francesco AM, Mazzuoli R, Poli G, Stanzione D (1989) Geochemistry of recent volcanics of Ischia Island, Italy: evidences of crystallization and magma mixing. Chem Geol 78:15–33

D'Antonio M, Tonarini S, Arienzo I, Civetta L, Di Renzo V (2007) Components and processes in the magma genesis of the Phlegrean Volcanic District, southern Italy. In: Beccaluva L, Bianchini G, Wilson M (eds) Cenozoic volcanism in the Mediterranean area, vol 418. Geol Soc Am Spec Pap. GSA, Boulder, CO, pp 203–220

De Gennaro M, Ferreri M, Ghiara MR, Stanzione D (1984) Geochemistry of thermal waters on the island of Ischia (Campania, Italy). Geothermics 13:361–374

Della Seta M, Marotta E, Orsi G, de Vita S, Sansivero F, Fredi P (2012) Slope instability induced by volcano-tectonics as an additional source of hazard in active volcanic areas: the case of Ischia island (Italy). Bull Volcanol 74:79–106

de Vita S, Sansivero F, Orsi G, Marotta E (2006) Cyclical slope instability and volcanism related to volcano-tectonism in resurgent calderas: the Ischia Island (Italy) case study. Eng Geol 86:148–165

de Vita S, Sansivero F, Orsi G, Marotta E, Piochi M (2010) Volcanological and structural evolution of the Ischia resurgent caldera (Italy) over the past 10 k.y. In: Groppelli G, Viereck-Goette L (eds) Stratigraphy and geology of volcanic areas, vol 464. Geol Soc Am Spec Pap. GSA, Boulder CO, pp 193–241

Di Girolamo P, Ghiara MR, Lirer L, Munno R, Rolandi G, Stanzione D (1984) Vulcanologia e petrologia Dei Campi Flegrei [Volcanology and petrology of the Phlegraean fields]. Boll Soc Geol It 103:349–413

Di Napoli R, Aiuppa A, Bellomo S, Busca L, D'Alessandro W, Gagliano Candela E, Longo M, Pecoraino G, Valenza M (2009) A model for Ischia hydrothermal system: evidences from the chemistry of thermal groundwaters. J Volcanol Geotherm Res 186:133–159

Domenico PA, Schwartz FW (1997) Physical and chemical hydrogeology, 2nd edn. Wiley, Chichester, UK

Fournier N, Moreau M, Robertson R (2010) Disappearance of a crater lake: implications for potential explosivity at Soufrière volcano, St Vincent, Lesser Antilles. Bull Volcanol 73:543–555

Harbaugh AW (2005) MODFLOW-2005, the U.S. Geological Survey modular ground-water model—the groundwater flow process. USGS Techniques and Methods 6-A16. US Geological Survey, Reston, VA

Hurwitz S, Johnston MJS (2003) Groundwater level changes in a deep well in response to a magma intrusion event on Kilauea Volcano, Hawaii. Geophys Res Lett 30:2173

Hurwitz S, Kipp KL, Ingebritsen SE, Reid ME (2003) Groundwater flow, heat transport, and water table position within volcanic edifices: implications for volcanic processes in the Cascade Range. J Geophys Res 108(B12):2557

Inguaggiato S, Pecoraino G, D'Amore F (2000) Chemical and isotopic characterisation of fluid manifestations of Ischia Island. J Volcanol Geotherm Res 99:151–178

ISTAT (2017) Movimento turistico in Italia anno 2016 [Tourist flow in Italy, year 2016]. https://www.istat.it/it/files//2017/10/movimento_2016_rettifica-1.pdf

Jensen ME, Burman RD, Allen RG (1990) Evapotranspiration and irrigation water requirements. ASCE manuals and reports on engineering practice, no. 70, ASCE, New York

Join JL, Folio JL, Robineau B (2005) Aquifers and groundwater within active shield volcanoes: evolution of conceptual models in the Piton de la Fournaise Volcano. J Volcanol Geotherm Res 147:187–201

Langevin CD, Shoemaker WB, Guo W (2003)MODFLOW-2000, the U.S. Geological Survey Modular Ground-Water Model: documentation of the SEAWAT-2000. Version with the Variable-Density Flow Process (VDF) and the Integrated MT3DMS Transport Process (IMT). US Geol Surv Open-File Rep 03-426 http://fl.water.usgs.gov/Abstracts/ofr03_426_langevin.html. Accessed November 2019

Molin P, Acocella V, Funiciello R (2003) Structural, seismic and hydrothermal features at the border of an active intermittent resurgent block: Ischia Island (Italy). J Volcanol Geotherm Res 121:65–81

Monti S (2004) Il termalismo tra passato e futuro [The spa market between past and future]. La Rassegna d'Ischia 25(1):3–12

Orsi G, Gallo G, Zanchi A (1991) Simple-shearing block resurgence in caldera depressions: a model from Pantelleria and Ischia. J Volcanol Geotherm Res 47:1–11

Orsi G, Gallo G, Heiken G, Wohletz K, Yu E, Bonani G (1992) A comprehensive study of the pumice formation and dispersal: the Cretaio Tephra of Ischia (Italy). J Volcanol Geotherm Res 53:329–354

Orsi G, de Vita S, di Vito M (1996) The restless resurgent Campi Flegrei nested caldera (Italy): constraints on its evolution and configuration. J Volcanol Geotherm Res 74:179–214

Panichi C, Bolognesi L, Ghiara MR, Noto P, Stanzione D (1992) Geothermal assessment of the island of Ischia (southern Italy) from isotopic and chemical composition of the delivered fluids. J Volcanol Geotherm Res 49:329–348

Paoletti V, Di Maio R, Cella F, Florio G, Mocka K, Roberti N, Secomandi M, Supper R, Fedi M, Rapolla A (2009) The Ischia Volcanic Island (southern Italy): inferences from potential field data interpretation. J Volcanol Geotherm Res 179:69–86

Paoletti V, D'Antonio M, Rapolla A (2013) The structural setting of the Ischia Island (Phlegrean Volcanic District, southern Italy): inferences from geophysics and geochemistry. J Volcanol Geotherm Res 249:155–173

Pinder GF, Jones JF (1969) Determination of the groundwater component of peak discharge from chemistry of total runoff. Water Resour Res 5:438–445

Piscopo V, Allocca V, Formica F (2000) Sustainable management of groundwater in Neapolitan volcanic areas, Italy. In: Sililo O et al (eds) Groundwater: past achievements and future challenge. Balkema, Rotterdam, pp 1011–1016

Regione Campania (2008) Acque termali della Campania [Thermal waters of Campania]. Grafica Sud, Casalnuovo Napoli, Italy

Reid ME, Sisson TW, Brien DL (2001) Volcano collapse promoted by hydrothermal alteration and edifice shape, Mount Rainier, Washington. Geology 29:779

Revil A, Finizola A, Ricci T, Delcher E, Peltier A, Barde-Cabusson S, Avard G, Bailly T, Bennati L, Byrdina S, Colonge J, Di Gangi F, Douillet G, Lupi M, Letort J, Tsang Hin Sun E (2011) Hydrogeology of Stromboli volcano, Aeolian Islands (Italy) from the interpretation of resistivity tomograms, self-potential, soil temperature and soil CO2 concentration measurements. Geophys J Int 186:1078–1094

Rumbaugh JO, Rumbaugh DB (2017) Groundwater vistas version 7 manual. Environmental Simulations, Leesport, PA

Santacroce R, Cristofolini R, La Volpe L, Orsi G, Rosi M (2003) Italian active volcanoes. Episodes 26:227–234

Sbrana A, Toccaceli RM (2011) Carta Geologica dell'Isola d'Ischia con note illustrative, scala 1:10000 [Geological map of the island of Ischia with illustrative notes, scale 1: 10,000]. Regione Campania, Naples

Scandone P (1979) Origin of the Tyrrhenian Sea and Calabrian Arc. Boll Soc Geol It 98:27–34

Shibata T, Akita F (2001) Precursory changes in well water level prior to the march, 2000 eruption of Usu Volcano, Japan. Geophys Res Lett 28:1799–1802

Tedesco D (1996) Chemical and isotopic investigations of fumarolic gases from Ischia island (southern Italy): evidences of magmatic and crustal contribution. J Volcanol Geotherm Res 74:233–242

Tibaldi A, Vezzoli L (1998) The space problem of caldera resurgence: an example from Ischia Island. Italy, Geologische Rundschau 87:53–66

Tibaldi A, Vezzoli L (2004) A new type of volcano flank failure: the resurgent caldera sector collapse, Ischia, Italy. Geophys Res Lett 31:L14605

Turc L (1954) The water balance of soils, relation between precipitation evaporation and flow. Ann Agronomiques 5:491–569

UNESCO (1991) Hydrology and water resources of small islands: a practical guide. UNESCO, Paris

Vezzoli L (1988) Island of Ischia. Quaderni de La Ricerca Scientifica 114, Rome

Vezzoli L, Principe C, Malfatti J, Arrighi S, Tanguy J-C, Le Goff M (2009) Modes and times of caldera resurgence: the <10 ka evolution of Ischia caldera, Italy, from high-precision archaeomagnetic dating. J Volcanol Geotherm Res 186:305–319